

# The Nucleon Polarizability Program at MAMI-A2

Garth Huber



Catholic University of America  
February 1, 2018

Supported by:



SAPPJ-2015-00023

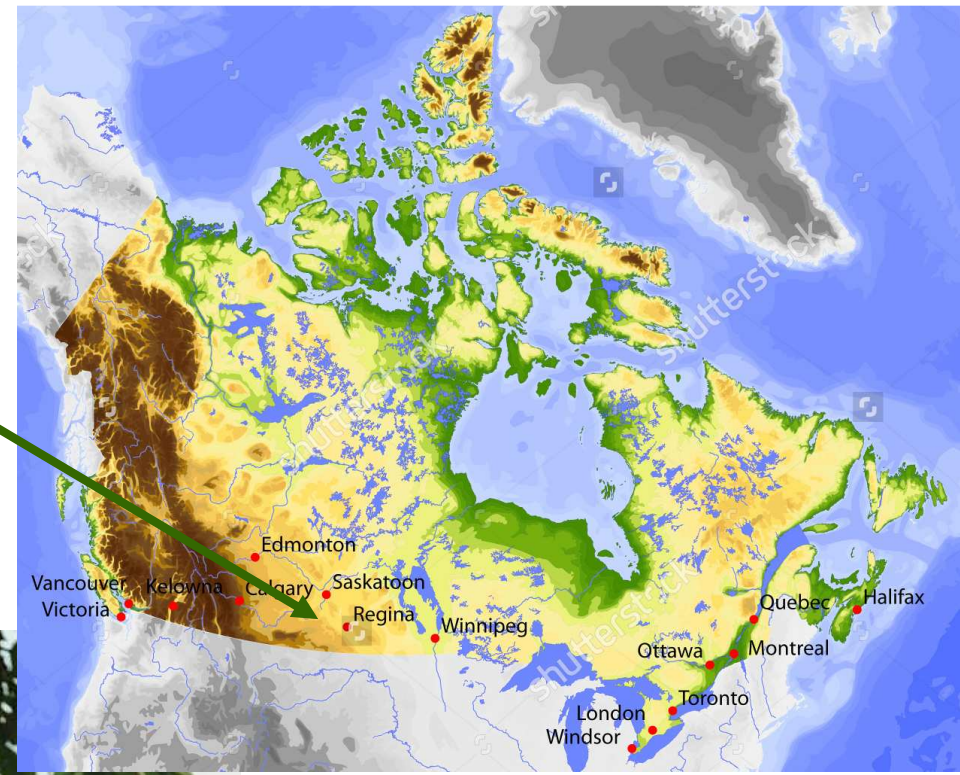
## Compton Working Group:

D. Hornidge, P. Martel (Mt. Allison), C. Collicott, A. Sarty (St. Mary's),  
R. Miskimen, A. Rajabi (U.Mass), E. Downie, V. Sokhoyan (GWU),  
Z. Ahmed, G.M. Huber, D. Paudyal (Regina),  
J. Annand (Glasgow), J. Arends (Mainz)





# Regina, Saskatchewan CANADA



Regina is named after Queen Victoria, and is capital of the province of Saskatchewan





University  
of Regina

- **Founded 1974.**
- **15,276 students, incl. ~2,000 Grad Students (2017).**
- **Physics Dept. offers B.Sc., M.Sc. and Ph.D. degrees.**

# Particle Data Group: Baryon Listings

**p**

$$I(J^P) = \frac{1}{2}(\frac{1}{2}^+) \text{ Status: } ****$$

**p MASS (MeV)**

VALUE (MeV)

**938.272013 ± 0.000023**

**p MAGNETIC MOMENT**

VALUE ( $\mu_N$ )

**2.792847356 ± 0.000000023**

Valence quarks: uud

**p CHARGE RADIUS**

VALUE (fm)

**0.8768 ± 0.0069**

**p ELECTRIC DIPOLE MOMENT**

VALUE ( $10^{-23}$  e cm)

**< 0.54**

**p ELECTRIC POLARIZABILITY  $\alpha_p$**

VALUE ( $10^{-4}$  fm<sup>3</sup>) DC

**12.0 ± 0.6 OUR AVERAGE**

**p MEAN LIFE**

LIMIT  
(years)

**> 5.8 × 10<sup>29</sup>**

**> 2.1 × 10<sup>29</sup>**

PARTICLE

**n**

**p**

**p DECAY MODES**

**p MAGNETIC POLARIZABILITY  $\beta_p$**

VALUE ( $10^{-4}$  fm<sup>3</sup>) DI

**1.9 ± 0.5 OUR AVERAGE**

*Response to a deformation force*

# What is a Polarizability?

A measure of response of system to a quasi-static field.

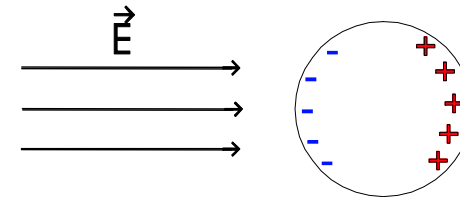
e.g. Electric Polarizability  $\alpha_E$

Applied  $E$  induces EDM

$$\vec{p} = \alpha_E \vec{E}$$

with energy density

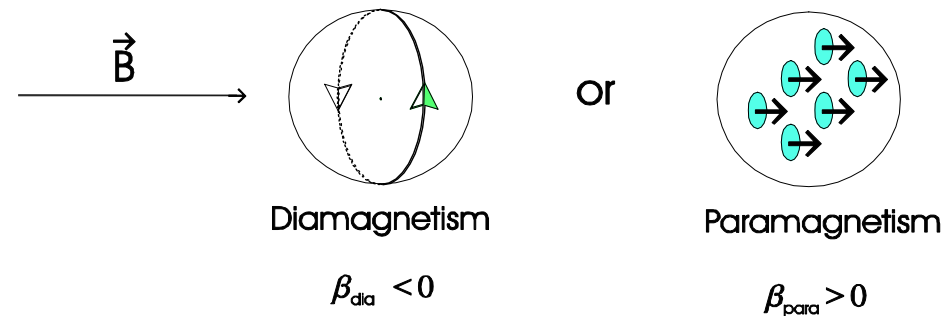
$$u_E = -\frac{1}{2} \alpha_E \vec{E}^2$$



Similarly, applied  $H$  induces MDM

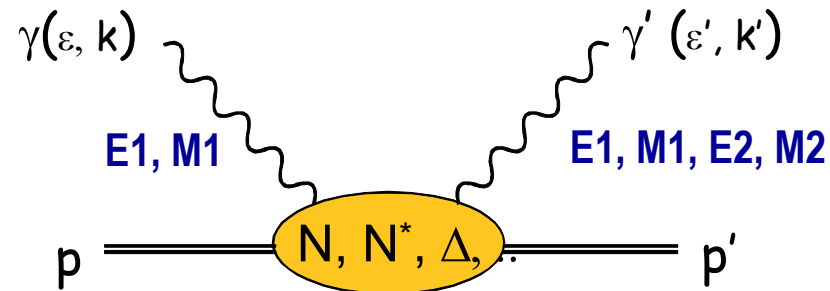
$$\vec{m} = \beta_M \vec{H}$$

$$u_M = -\frac{1}{2} \beta_M \vec{H}^2$$





# Nucleon Scalar Polarizabilities



Low energy outgoing photon plays role of applied E.M. dipole field

Nucleon response:  
**POLARIZABILITIES**

## Nucleon Polarizabilities of interest to many fields:

- In astrophysics, they determine neutron star properties.
- In atomic physics, they yield an appreciable correction to Lamb shift and hyperfine structure.
- Uncertainty in scalar polarizability is the largest uncertainty in proton radius extraction from H excitation spectrum

# How to measure Proton Scalar Polarizabilities

- Accessed via Compton scattering of Real Photons



- 2<sup>nd</sup> and higher order terms describe polarizabilities and evidence of proton's internal structure.

$$H_{eff}^{(2)} = \frac{1}{2} \alpha_{E1} \vec{E}^2 + \frac{1}{2} \beta_{M1} \vec{H}^2$$

- Compton scattering angular distribution

$$\frac{d\sigma}{d\Omega} = \frac{\alpha^2}{m^2} \left( \frac{\omega'}{\omega} \right)^2 \left( \frac{1}{2} (1 + \cos^2 \theta) - \frac{m\omega\omega'}{\alpha} \left[ \frac{\alpha_{E1} + \beta_{M1}}{2} (1 + \cos \theta)^2 + \frac{\alpha_{E1} - \beta_{M1}}{2} (1 - \cos \theta)^2 + \dots \right] \right)$$

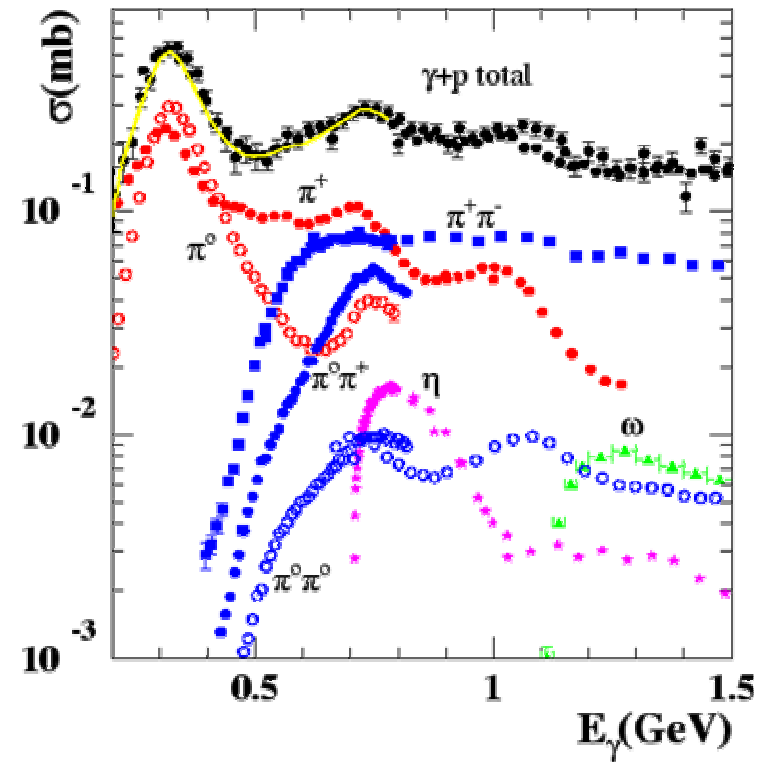


## 1. Total inclusive photoabsorption cross section:

$$\alpha_{E1} + \beta_{M1} = \frac{1}{2\pi^2} \int_{\nu_{thr}}^{\infty} \frac{d\nu}{\nu^2} \sigma_{abs}(\nu)$$

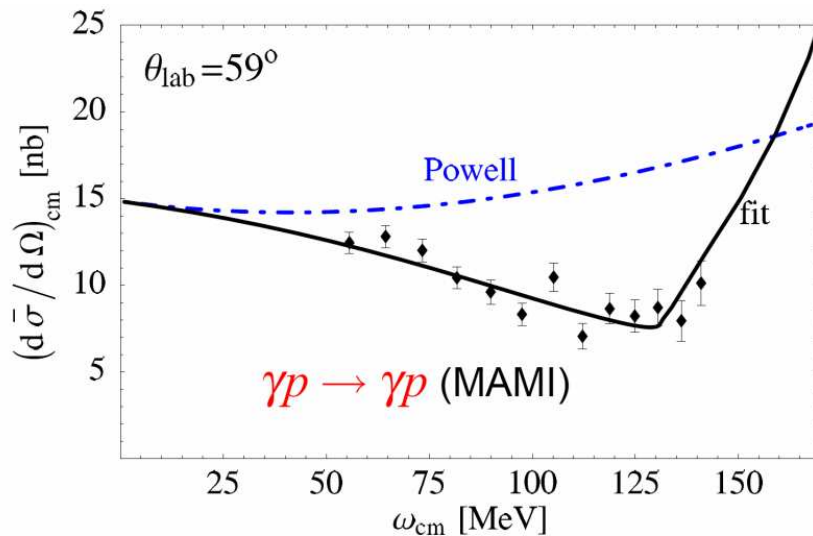
Baldin Sum Rule (1960)

**Sum Rule is model independent**  
 → but a model is needed to  
 evaluate integral beyond  
 experimental data.



$$\alpha_{E1} + \beta_{M1} = (13.8 \pm 0.4) \cdot 10^{-4} \text{ fm}^3$$

## 2. Compton scattering angular distribution vs energy ( $\nu$ )



Olmos de Leon et al., EPJ A10 (2001)

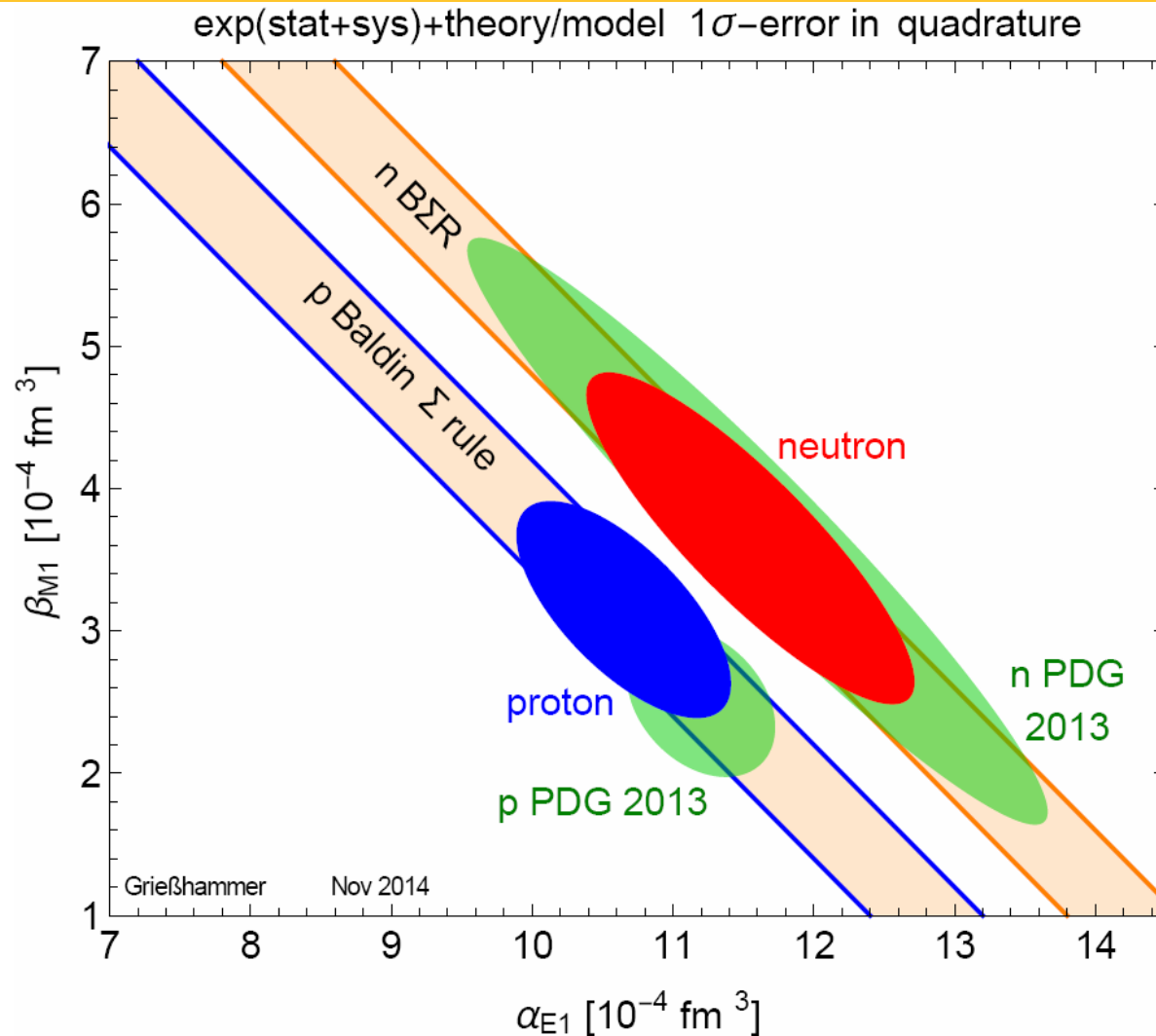
**Powell cross section:** photon scattering off a pointlike nucleon with anomalous magnetic moment.

**Dispersion relation analysis** used to extract  $\alpha$   $\beta$  from the data.

$$\alpha_{E1} - \beta_{M1} = (10.5 \pm 0.9) \cdot 10^{-4} \text{ fm}^3$$

# Global Analysis of Compton Data Constraints

H.W. Griesshammer, Priv. Comm. (2015)



- Electric polarizability  $\alpha_{E1}$  well constrained by experimental data.
- Magnetic polarizability  $\beta_{M1}$  less certain.
  - Diamagnetism is important in the nucleon, but uncertainty  $\sim 25\%$ .
- Neutron data are particularly uncertain.



# A simple picture of what the results mean

## Experimental values (PDG2014):

$$\alpha_{E1} = (11.2 \pm 0.4) \times 10^{-4} \text{ fm}^3 \quad \beta_{M1} = (2.5 \pm 0.4) \times 10^{-4} \text{ fm}^3$$

## Size of $\alpha_{E1}$ measures “stiffness” of system to electric deformation.

- For  ${}^1\text{H}$  atom, expect:

$$\alpha_E^H = \frac{9}{2} a_B^3 = \frac{27}{8\pi} \text{ Vol}$$

- But proton data indicate:

$$\alpha_E^P \cong 3 \times 10^{-4} \text{ Vol}$$

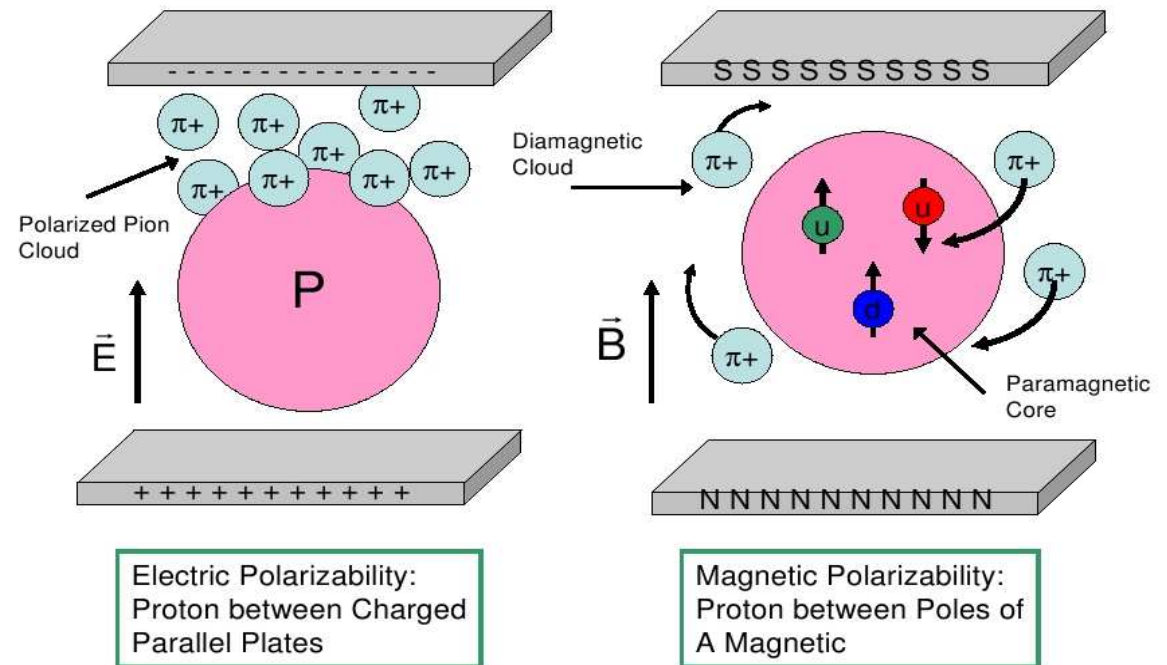
- The proton is very “stiff”, because:

$$\frac{\alpha_E^P}{\alpha_E^H} \approx \frac{E_{bind}^H}{E_{bind}^P} \approx \frac{\alpha_{EM}^2}{\alpha_{Strong}^2} \approx 10^{-4}$$

# More detailed explanation

- Need to take into account that the proton is surrounded by a virtual meson cloud in order to quantitatively understand the observed  $\alpha_{E1}$ ,  $\beta_{M1}$  polarizabilities.

- $p(J=1/2) \rightarrow \Delta(J=3/2)$  dipole transition makes very strong paramagnetic contribution to  $\beta_M \sim 10^{-3} \text{ fm}^3$ .
- Partially offset by strong diamagnetic component from meson cloud.



B. Holstein, MAMI and Beyond Conference, 2008.

# How to obtain more accurate values of $\alpha_{E1}$ , $\beta_{M1}$

- Desire for more precise proton  $\beta_{M1}$  has motivated a new generation of experiments.
- Combinations of cross sections with **linearly polarized photon beam**
  - Leading order contribution from  $\alpha$  and  $\beta$

$$\frac{d\sigma^{\parallel}}{d\Omega} = \frac{d\sigma_{Powell}^{\parallel}}{d\Omega} - \frac{e^2}{2\pi m_p} \left(\frac{v'}{v}\right)^2 v v' (\alpha_{E1} \cos^2 \theta + \beta_{M1} \cos \theta) + O(v^3)$$

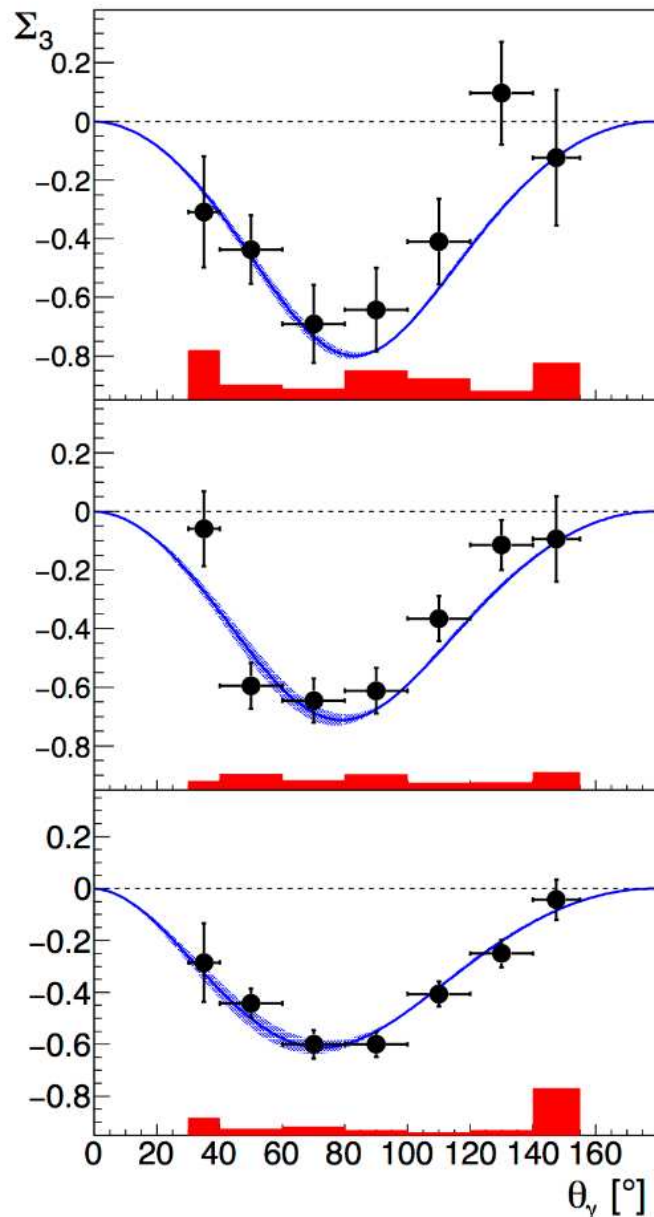
$$\frac{d\sigma^{\perp}}{d\Omega} = \frac{d\sigma_{Powell}^{\perp}}{d\Omega} - \frac{e^2}{2\pi m_p} \left(\frac{v'}{v}\right)^2 v v' (\alpha_{E1} + \beta_{M1} \cos \theta) + O(v^3)$$

- **New work by Krupina & Pascalutsa [PRL 110 262001 (2013)]**  
→ At low energies, use beam asymmetry  $\Sigma_3$  to extract  $\beta_{M1}$

$$\begin{aligned}\Sigma_3 &\equiv \frac{d\sigma^{\perp} - d\sigma^{\parallel}}{d\sigma^{\perp} + d\sigma^{\parallel}} \\ &= \Sigma_3^{Born} - f_3(\theta) \beta_{M1} v^2 + O(v^4)\end{aligned}$$



# Pioneering $\alpha_{E1}$ , $\beta_{M1}$ from $\Sigma_3$ Asymmetry



84 MeV

108 MeV

129 MeV

First use of linearly polarized photon beam asymmetry  $\Sigma_3$  below pion threshold to determine proton magnetic polarizability.

Fit results using BChPT gives:

$$\beta_{M1} = 2.8_{-2.1}^{+2.3} \times 10^{-4} \text{ fm}^3$$

- Only 1/3 of approved data taken so far:
- New data run with upgraded photon tagger focal plane with drastically reduce the statistical uncertainties.

# Proton Spin (Vector) Polarizabilities

To include spin, next term in Hamiltonian:

$$H_{eff}^{(3)} = -\frac{1}{2} \left[ \gamma_{E1E1} \vec{\sigma} \cdot \vec{E} \times \dot{\vec{E}} + \gamma_{M1M1} \vec{\sigma} \cdot \vec{H} \times \dot{\vec{H}} \right. \\ \left. + 2\gamma_{E1M2} H_{ij} \sigma_i E_j - 2\gamma_{M1E2} E_{ij} \sigma_i H_j \right]$$

involves one field derivative wrt either time or space  $\dot{\vec{E}} = \partial_t \vec{E}$ ,  $E_{ij} = \frac{1}{2} (\nabla_i E_j + \nabla_j E_i)$

e.g.  $\gamma_{M1E2}$  excited by electric quadrupole (E2) radiation  
and decays by magnetic dipole (M1) radiation

- **“Stiffness” of proton spin against E.M.-induced deformations relative to the spin axis.**
  - Defines the frequency of proton’s spin precession induced by variable E.M. fields.
  - Higher order in incident proton energy, small effect at lower energies.
- Each spin polarizability is dominated by a pion-pole contribution.
  - The dispersive (interesting) part is relatively small.

# Proton Spin Polarizability Predictions

	Kmat	HDPV	DPV	$L_\chi$	HB $\chi$ PT	B $\chi$ PT
$\gamma_{E1E1}$	-4.8	-4.3	-3.8	-3.7	$-1.1 \pm 1.8$ (th)	-3.3
$\gamma_{M1M1}$	3.5	2.9	2.9	2.5	$2.2 \pm 0.5$ (st) $\pm 0.7$ (th)	3.0
$\gamma_{E1M2}$	-1.8	-0.0	0.5	1.2	$-0.4 \pm 0.4$ (th)	0.2
$\gamma_{M1E2}$	1.1	2.2	1.6	1.2	$1.9 \pm 0.4$ (th)	1.1
$\gamma_0$	2.0	-0.8	-1.1	-1.2	-2.6	-1.0
$\gamma_\pi$	11.2	9.4	7.8	6.1	5.6	7.2

Spin polarizabilities in units of  $10^{-4} \text{fm}^4$ .  
Pion Pole Subtracted.

## K-matrix:

Kondratyuk et al., PRC 64, 024005 (2001)

## HDPV, DPV (Dispersion Relation):

Holstein et al., PRC 61, 034316 (2000)

Drechsel et al., Phys.Rep. 378, 99 (2003)

Pasquini et al., PRC 76, 015203 (2007)

## $L_\chi$ (Chiral Lagrangian):

Gasparyan et al., NP A866, 79 (2011)

## HB $\chi$ PT, B $\chi$ PT (Heavy Baryon & Covariant Chiral PT):

McGovern et al., EPJ A49, 12 (2013)

Lensky et al, PRC 89, 032202 (2014)



One can extract the spin polarizabilities using knowledge of  $\alpha_{E1}$ ,  $\beta_{M1}$ , the linear combinations  $\gamma_0, \gamma_\pi$ , and Subtracted Dispersion Relations.

## Backward Spin Polarizability (unpolarized Compton scattering)

$$\gamma_\pi = \gamma_{E1E1} + \gamma_{M1M1} - \gamma_{E1M2} + \gamma_{M1E2}$$

$$\gamma_\pi = (-38.7 \pm 1.8) \cdot 10^{-4} \text{ fm}^4$$

Schumacher, Prog. Part. Nucl. Phys. **55**, 567(2005)

**Pion pole contributes -46.7**

**Dispersive part  $8.0 \pm 1.8$  known only to  $\approx 25\%$ .**

## Forward Spin Polarizability (polarized beam and target)

$$\gamma_0 = -\gamma_{E1E1} - \gamma_{M1M1} - \gamma_{E1M2} - \gamma_{M1E2}$$

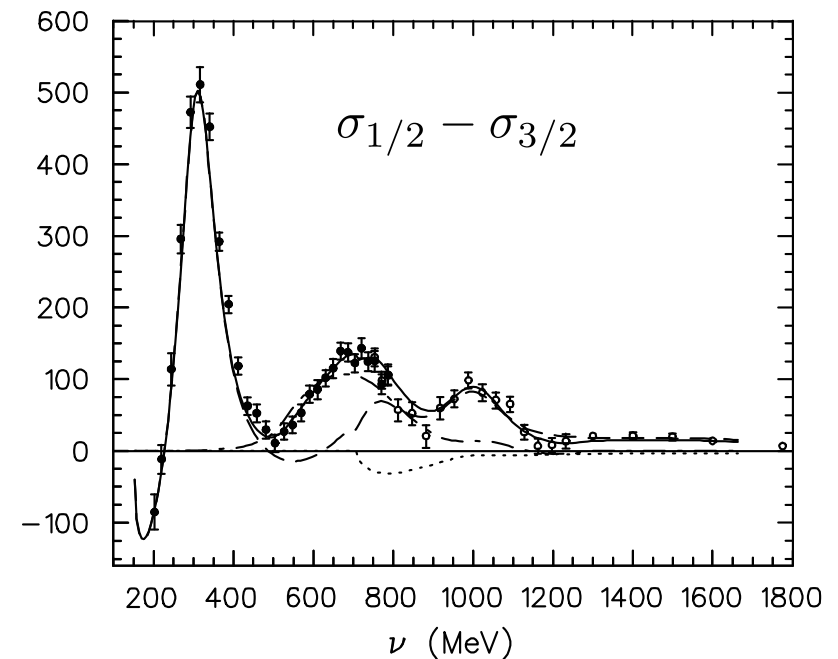
$$\gamma_0 = \frac{1}{4\pi^2} \int_{\nu_{thr}}^{\infty} \frac{\sigma_{1/2} - \sigma_{3/2}}{\nu^3} d\nu$$

$$\gamma_0 = -(1.00 \pm 0.08 \pm 0.10) \times 10^{-4} \text{ fm}^4$$

Ahrens et al., PRL**87**, 022003 (2001)

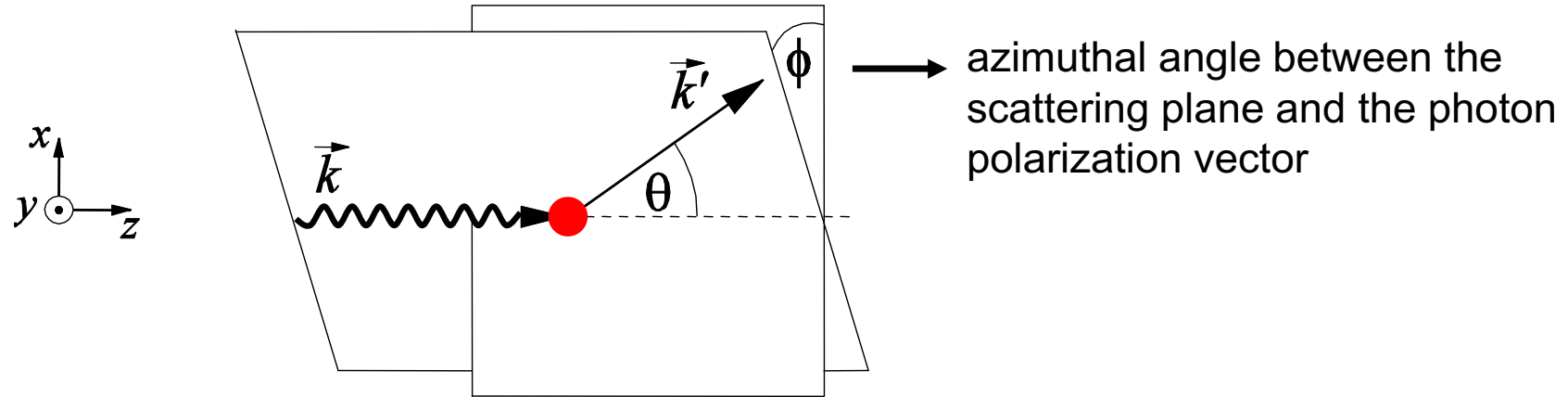
**Known to  $\approx 10\%$ .**

**Pion pole contribution cancels.**



- **Spin polarizabilities appear in the effective interaction Hamiltonian at third order in photon energy**
  - It is in the  $\Delta$  resonance region ( $E_\gamma=200-300$  MeV) where their effect becomes significant.
- **In this energy region, it is possible to accurately measure polarization asymmetries using a variety of polarized beam and target combinations**
  - The various asymmetries respond differently to the individual spin polarizabilities at different  $E_\gamma$  and  $\theta$ .
  - Measure three asymmetries at different  $E_\gamma, \theta$ .
- **Then conduct a global analysis:**
  - Include constraints from “known”  $\gamma_0, \gamma_\pi, \alpha_{E1}, \beta_{M1}$ .
  - Extract all four spin polarizabilities independently with small statistical, systematic and model-dependent errors.

# Asymmetries with Linearly Polarized $\gamma$



- $\phi = 0$  and unpolarized target  $\rightarrow \Sigma_3$
- $\phi = 0$  and transversely polarized target in the y direction  $\rightarrow \Sigma_{3y}$
- $\phi = 45^\circ$  and longitudinally pol. target  $\rightarrow \Sigma_{1z}$
- $\phi = 45^\circ$  and transv. pol. target in the x direction  $\rightarrow \Sigma_{1x}$

$$\Sigma_3 = \frac{\sigma_{\parallel} - \sigma_{\perp}}{\sigma_{\parallel} + \sigma_{\perp}}$$

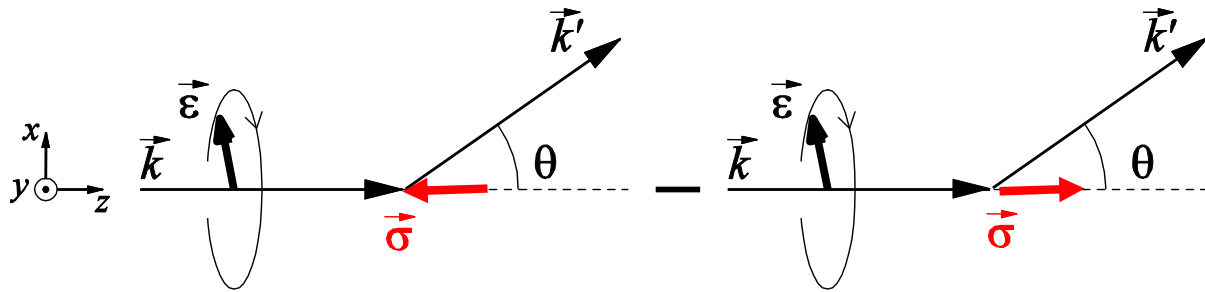
Asymmetry is measured with linearly polarized photons, parallel and perpendicular to the scattering plane, and unpolarized target.



# Double Spin Asymmetries w/ Circularly Polarized $\gamma$

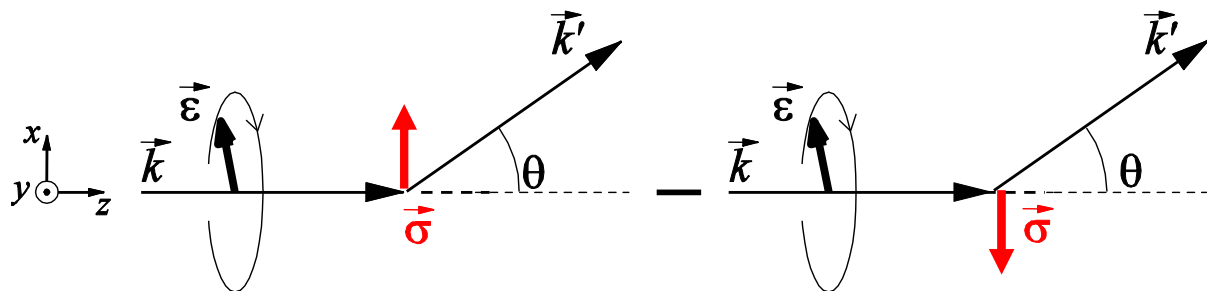
## ❖ Longitudinal asymmetry

$$\left[ \Sigma_{2z} = \frac{\left( \frac{d\sigma}{d\Omega} \right)_{\uparrow\uparrow} - \left( \frac{d\sigma}{d\Omega} \right)_{\uparrow\downarrow}}{\text{Sum}} \right]_{h=\pm 1}$$



## ❖ Transverse asymmetry

$$\left[ \Sigma_{2x} = \frac{\left( \frac{d\sigma}{d\Omega} \right)_{\uparrow\rightarrow} - \left( \frac{d\sigma}{d\Omega} \right)_{\uparrow\leftarrow}}{\text{Sum}} \right]_{h=\pm 1}$$



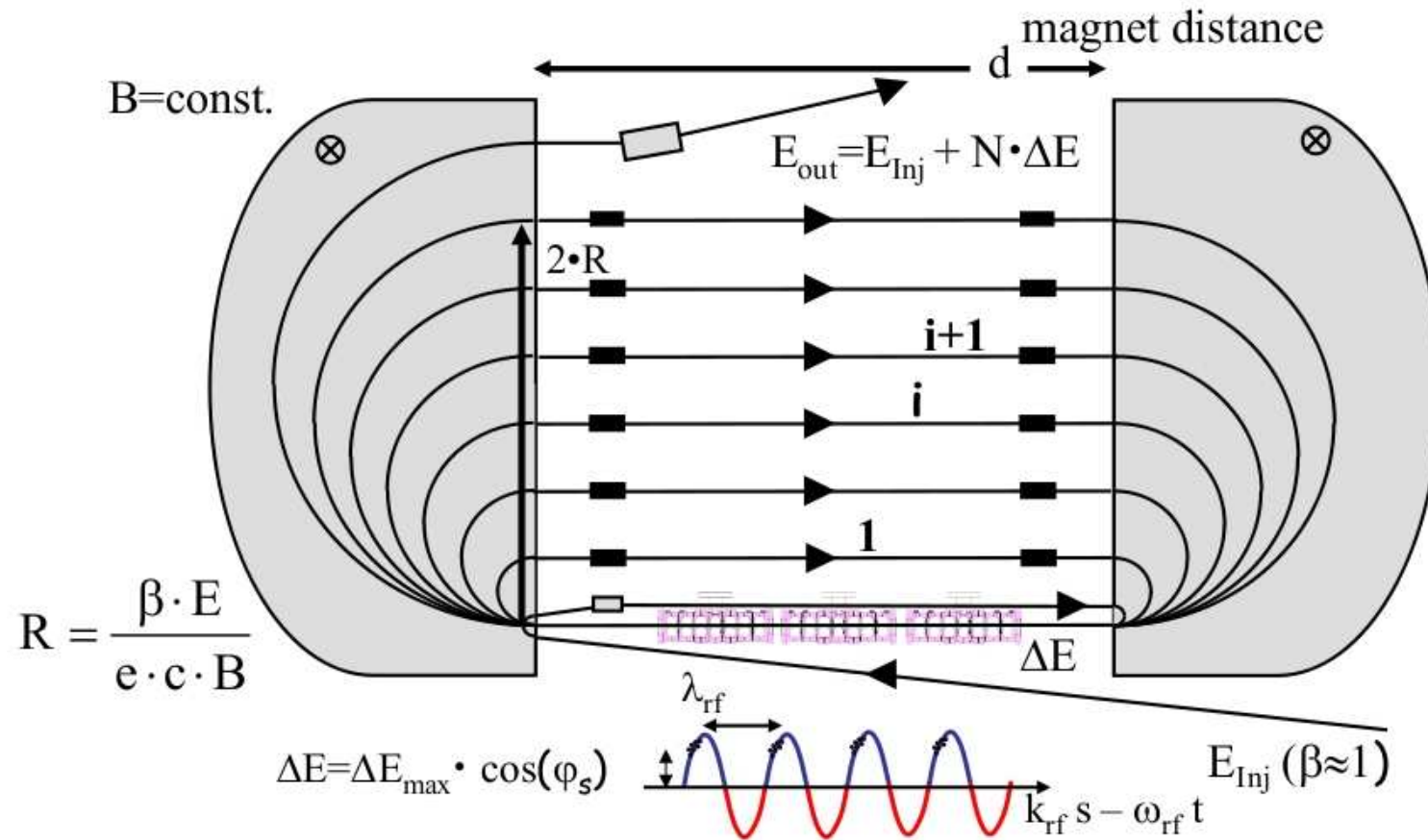
# Sensitivity to Spin Polarizabilities

	Polarization			
Polarization Asymmetry	Beam	Target	$E_\gamma$ Range (MeV)	Spin Polarizability
$\Sigma_{2z}$	Circular	Longitudinal	200 300	$\gamma_{M1M1}$
$\Sigma_{2x}$		Transverse	200 300	$\gamma_{E1E1}$
$\Sigma_3$	Linear	None	200 300	$\gamma_{M1M1}$
$\Sigma_{3y}$		Transverse	200 300	$\gamma_{E1E1}$
$\Sigma_{1z}$		Longitudinal	200 300	Both
$\Sigma_{1x}$		Transverse	150 250	Both



- Major facility upgrade in 2000's:
  - Upgraded accelerator.
  - Upgraded detectors.
  - New frozen spin target.
- “Ultimate” polarized observables laboratory:
  - polarized beam.
  - polarized target.
  - recoil polarization.
- Nearly  $4\pi$  Detector Coverage.





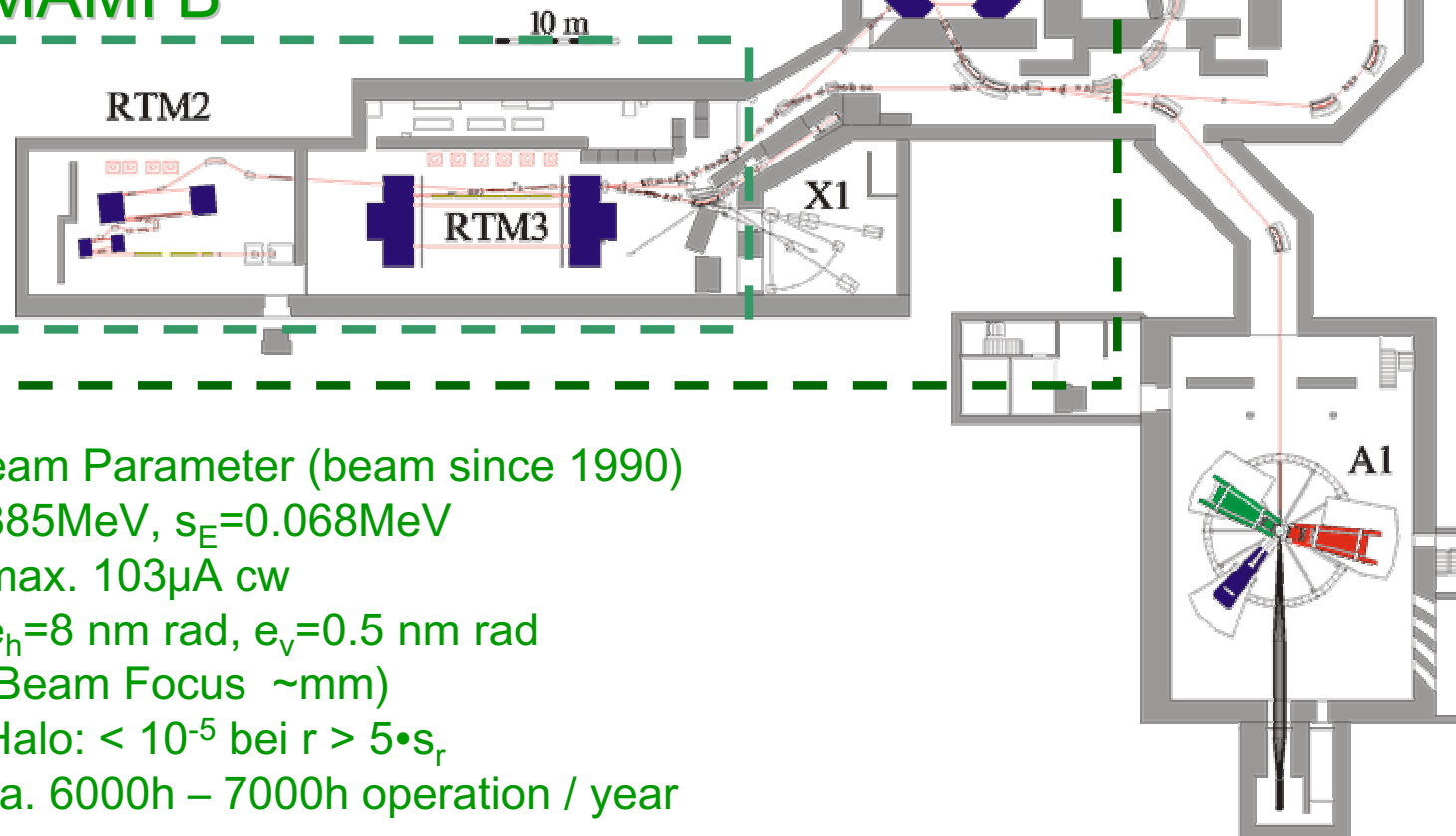
- ◆ 2 m long, 25 kW Hf, 18 MeV acceleration
- ◆ Need 1km Linac to get 800 MeV
- ◆ Solution → multiple passes! → Race Track Microtron (RTM)

## MAMI C

Parameter (Oct 2009)

- 1604MeV,  $s_E=0.100\text{MeV}$
- max. 100 $\mu\text{A}$
- $e_h=9\text{ nm rad}$ ,  $e_v=0.5\text{ nm rad}$   
as MAMI B !

## MAMI B



Beam Parameter (beam since 1990)

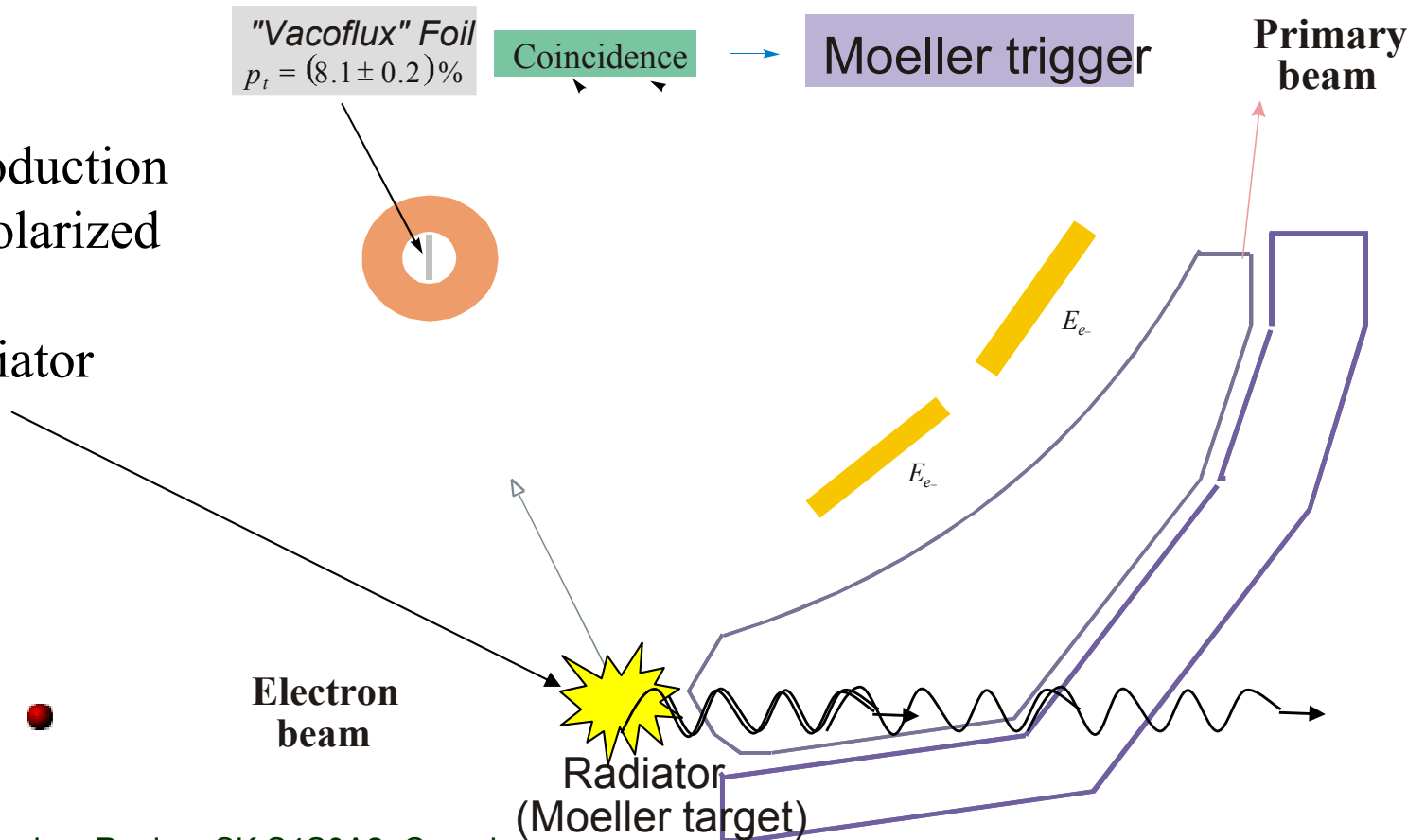
- 885MeV,  $s_E=0.068\text{MeV}$
- max. 103 $\mu\text{A}$  cw
- $e_h=8\text{ nm rad}$ ,  $e_v=0.5\text{ nm rad}$   
(Beam Focus  $\sim\text{mm}$ )
- Halo:  $< 10^{-5}$  bei  $r > 5 \cdot s_r$
- ca. 6000h – 7000h operation / year

1. Production and energy measurement of Bremsstrahlung photons

2. Determination of the degree of polarization of the electron beam (Moeller Polarimeter);  
Circularly pol. photons

$$A = \frac{N^+ - N^-}{N^+ + N^-} = a \vec{p}_t \vec{p}_b \cos(z)$$

3. Coherent production of linearly polarized photons on a diamond radiator



Energy resolution of our standard tagger ladder (352 plastics) **4 MeV per Channel.**

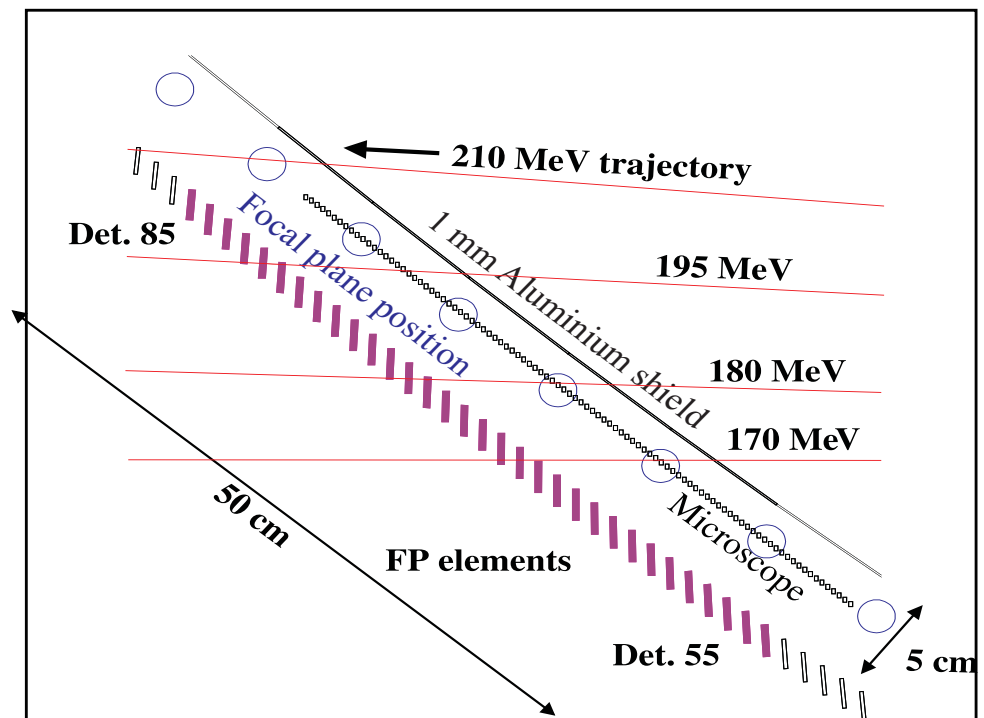
- **96 Plastic Scintillator**

Fibers (3x2 mm).

- 1/3 Overlap of the fibers with its neighbor. Overlap region defines the Microscope channel  **$\mu ch$  (191 channels)**.

- Energy resolution: **0.3 MeV per microscope channel ( $\mu ch$ )**.

- Microscope Tagger is positioned in the electron energy range of the reaction threshold,  
e.g. Beam energy  $E_0=883$  MeV corresponds to a **photon energy range from 674 MeV to 730 MeV** ( $\eta$ -threshold  $\sim 707$  MeV).





## TAPS:

366 BaF<sub>2</sub>, 72 PbWO<sub>4</sub> elements

384 Veto paddles

Max. kin. energy:

$\pi^{+-}$  : 180 MeV

$K^{+-}$  : 280 MeV

P : 360 MeV

## Crystal Ball:

672 NaI detectors

Max. kin. energy:

$\mu^{+-}$  : 233 MeV

$\pi^{+-}$  : 240 MeV

$K^{+-}$  : 341 MeV

P : 425 MeV

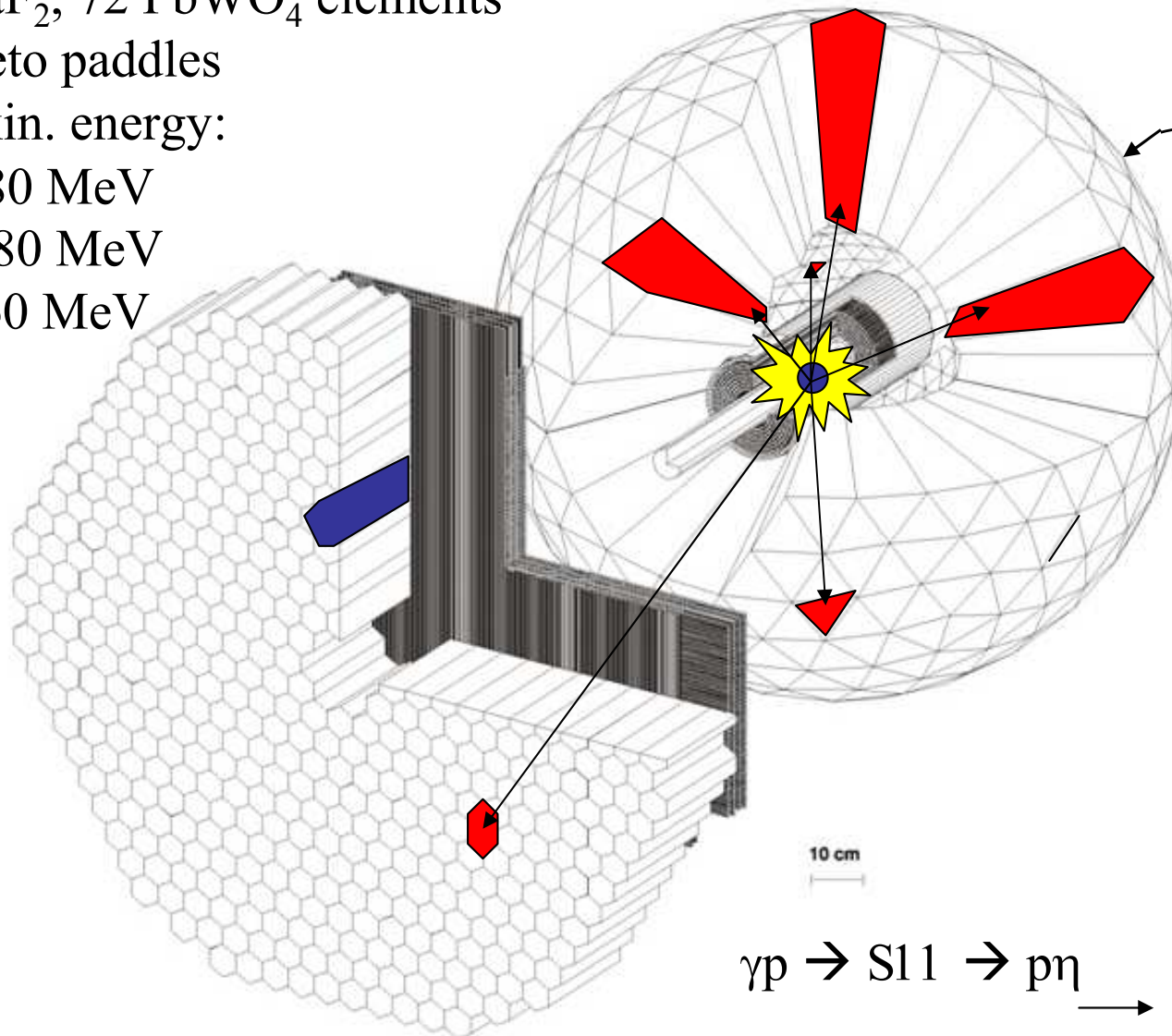
## Vertex detector:

2 Cylindr. MWPCs

480 wires, 320 stripes

## PID detector:

24 thin plastic detectors



$\gamma p \rightarrow S11 \rightarrow p\eta$

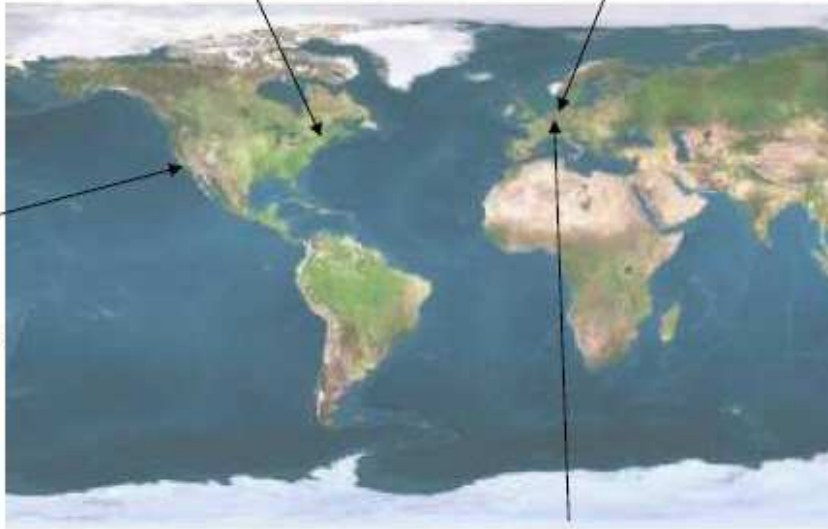
$\longrightarrow \pi^0\pi^0\pi^0$

$\longrightarrow \gamma\gamma\gamma\gamma\gamma\gamma$

1996-2002  
BNL-AGS  
( $E_{cm} = 1.2 - 1.53 \text{ GeV}$ )  
 $N^*$ ,  $\Delta$ ,  $\Lambda^*$ ,  $\Sigma$ ,  
 $\eta$  decays, medium. mod

1982-1986  
DORIS  
( $E_{cm} = 9 - 10 \text{ GeV}$ )  
 $\Upsilon$  spectroscopy  
radiative  $\Upsilon$  decays

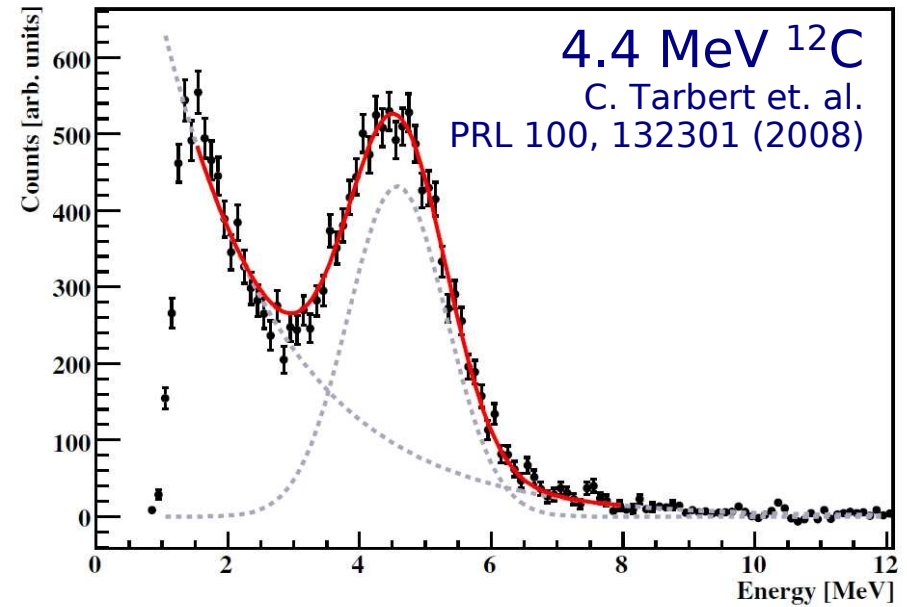
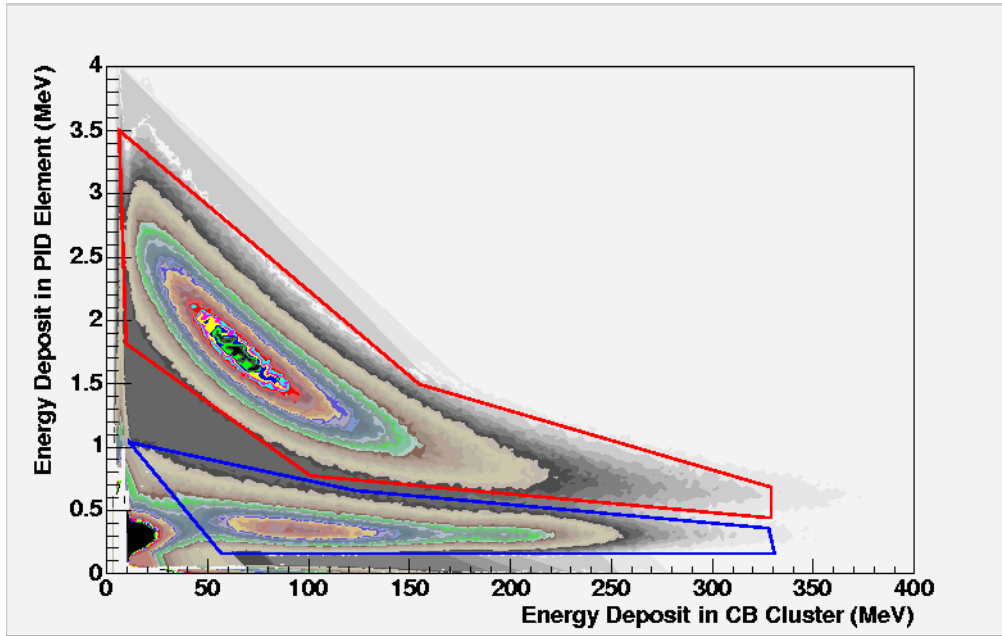
1976  
Conceived  
1978 - 1981  
SPEAR  
( $E_{cm} = 3 - 7 \text{ GeV}$ )  
 $\psi, \psi'$  spectroscopy  
radiative  $\phi$  decays  
 $\tau$  decays  
D decays,  
 $\Upsilon \rightarrow \gamma \Upsilon$ ,  
 $\eta, \eta', f$



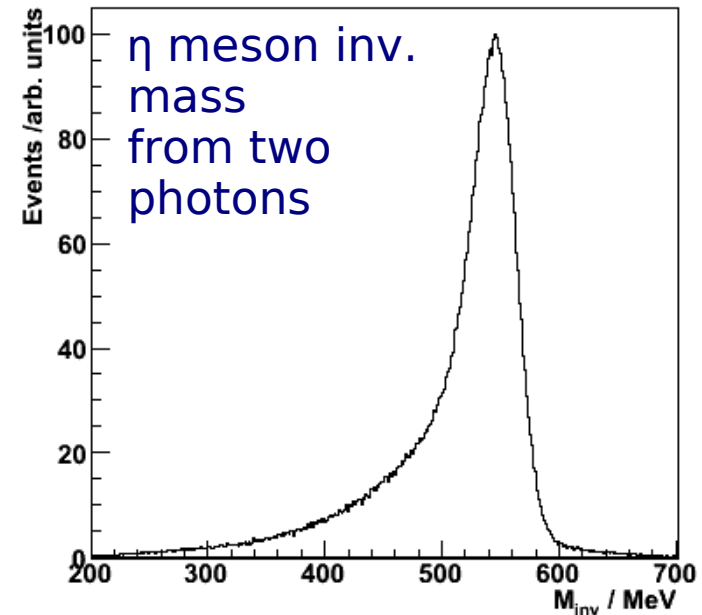
2002  
MAMI  
( $E_{cm} = 1.2 - 1.9 \text{ GeV}$ )



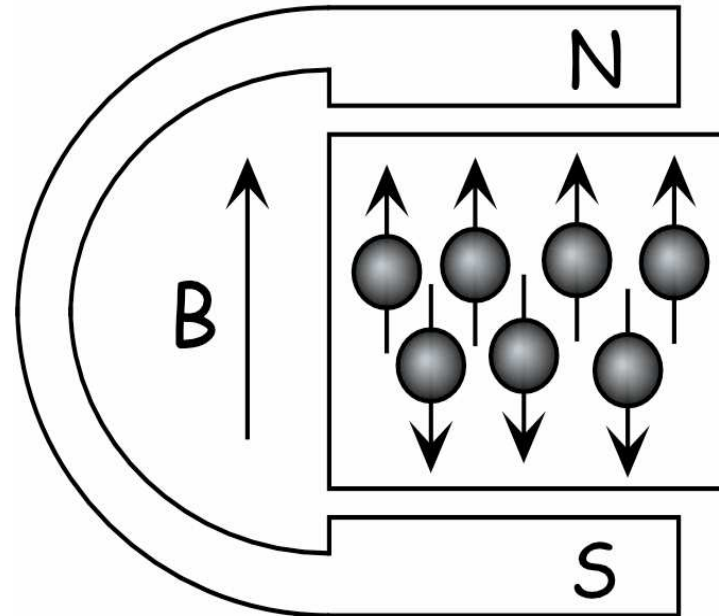
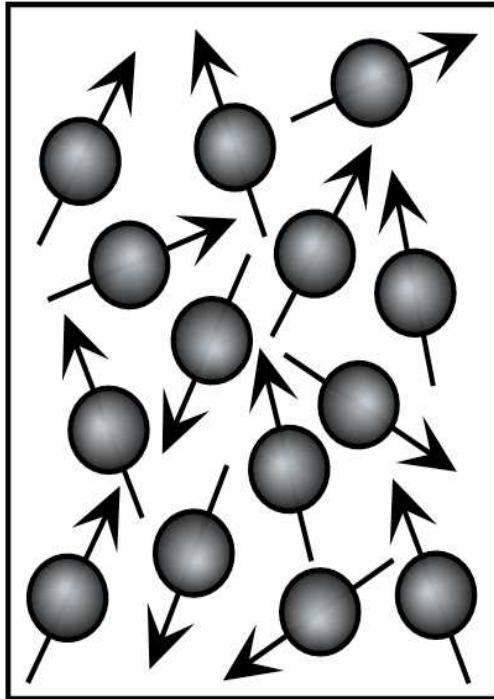
- ◆ Accurate separation of final states → good detector resolution.
- ◆ Sensitivity to small  $\sigma$  processes →  $4\pi$  detector acceptance, large  $\gamma$  flux.
- ◆ Access to polarization observables → polarized beam, target, recoil.



- ◆ Wide energy range with good resolution
- ◆ Energy resolution:  $\Delta E/E = 0.020 \cdot E[\text{GeV}]^{0.36}$
- ◆ Angular resolution:  $\sigma_\theta = 2 \quad 3\sigma_\varphi = \sigma_\theta / \sin(\theta)$
- ◆ MWPC → Charged particle tracking
- ◆  $\Delta E$  (PID) /  $E$  (CB) locus → particle id.
- ◆ High photon & neutron efficiency



Polarization = Orientation of Spins in a magnetic field



$$P = \frac{N\uparrow - N\downarrow}{N\uparrow + N\downarrow}$$

P=100% is not so easy to realize: Complicated interplay between

Polarizing force

~  
and

magnetic field **B**

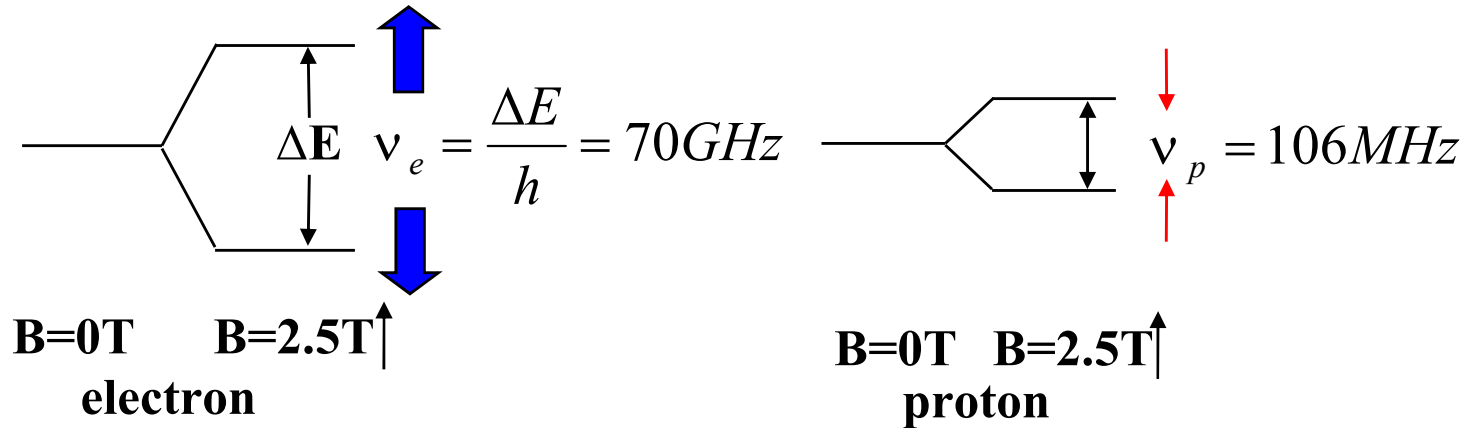
Depolarizing force

~

thermal motion of spins  
(temperature **T** – relaxation)



Magnetic moment in magnetic field:  $E = -\vec{\mu} \cdot \vec{B} = -g\mu_o mB$



Thermal equilibrium  
Boltzmann distribution

$$\frac{N(E + \Delta E)}{N(E)} = e^{-\frac{\Delta E}{kT}}$$

Spin 1/2

$$P = \frac{N_+ - N_-}{N_+ + N_-} = \tanh \frac{\mu B}{kT}$$

**T=1K**    **B=5T**    ➡    **P<sub>e</sub>=99.76%**    **P<sub>p</sub>=0.51%**

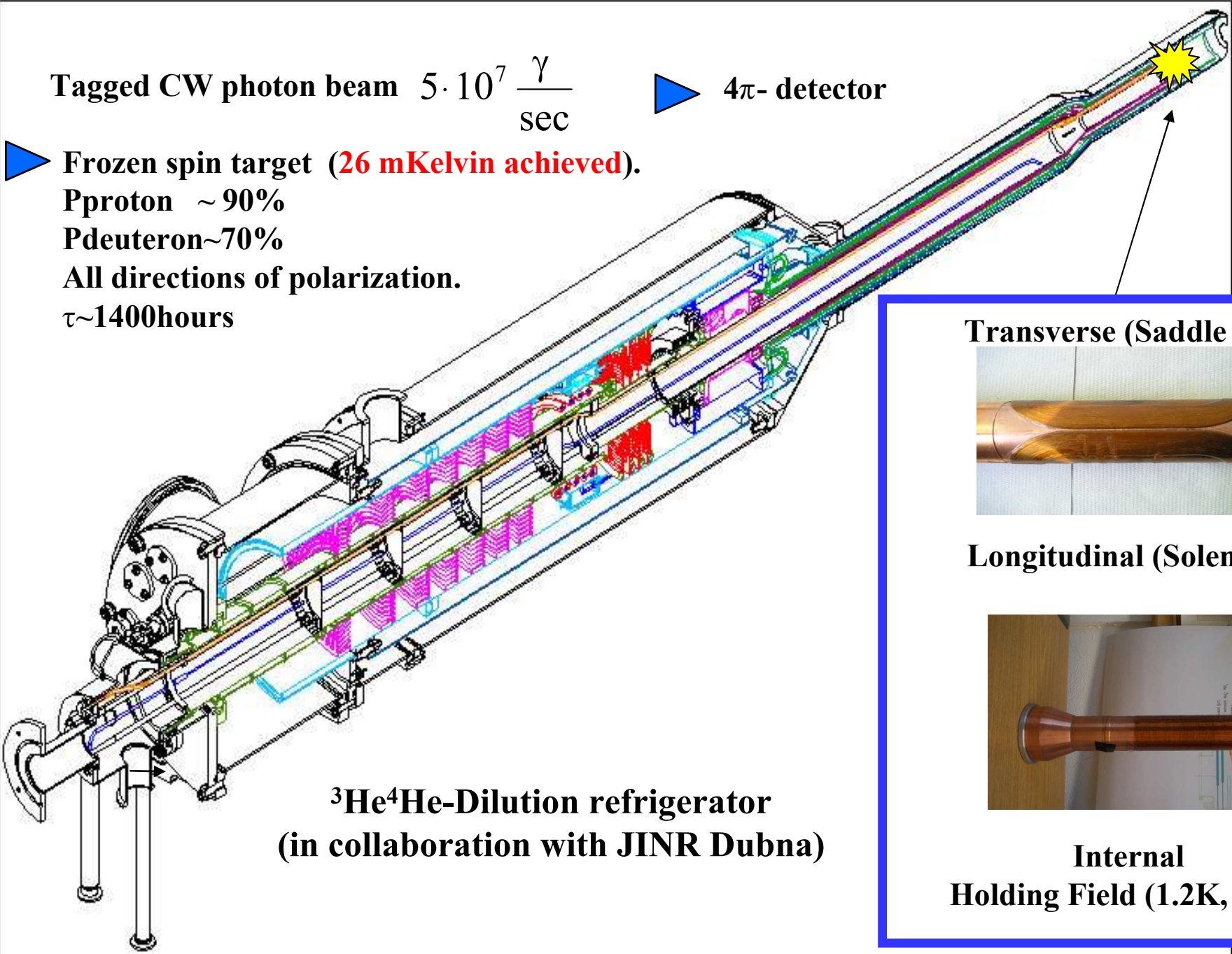
**Trick:** Transfer the high electron polarization to the nucleon via  $\mu$ -wave irradiation (DNP)

# Polarized Target for Crystal Ball

Tagged CW photon beam  $5 \cdot 10^7 \frac{\gamma}{\text{sec}}$

▶  $4\pi$ - detector

- ▶ Frozen spin target (**26 mKelvin achieved**).
- P<sub>proton</sub> ~ 90%
- P<sub>deuteron</sub> ~ 70%
- All directions of polarization.
- $\tau \sim 1400$  hours



**$^3\text{He}^4\text{He}$ -Dilution refrigerator  
(in collaboration with JINR Dubna)**

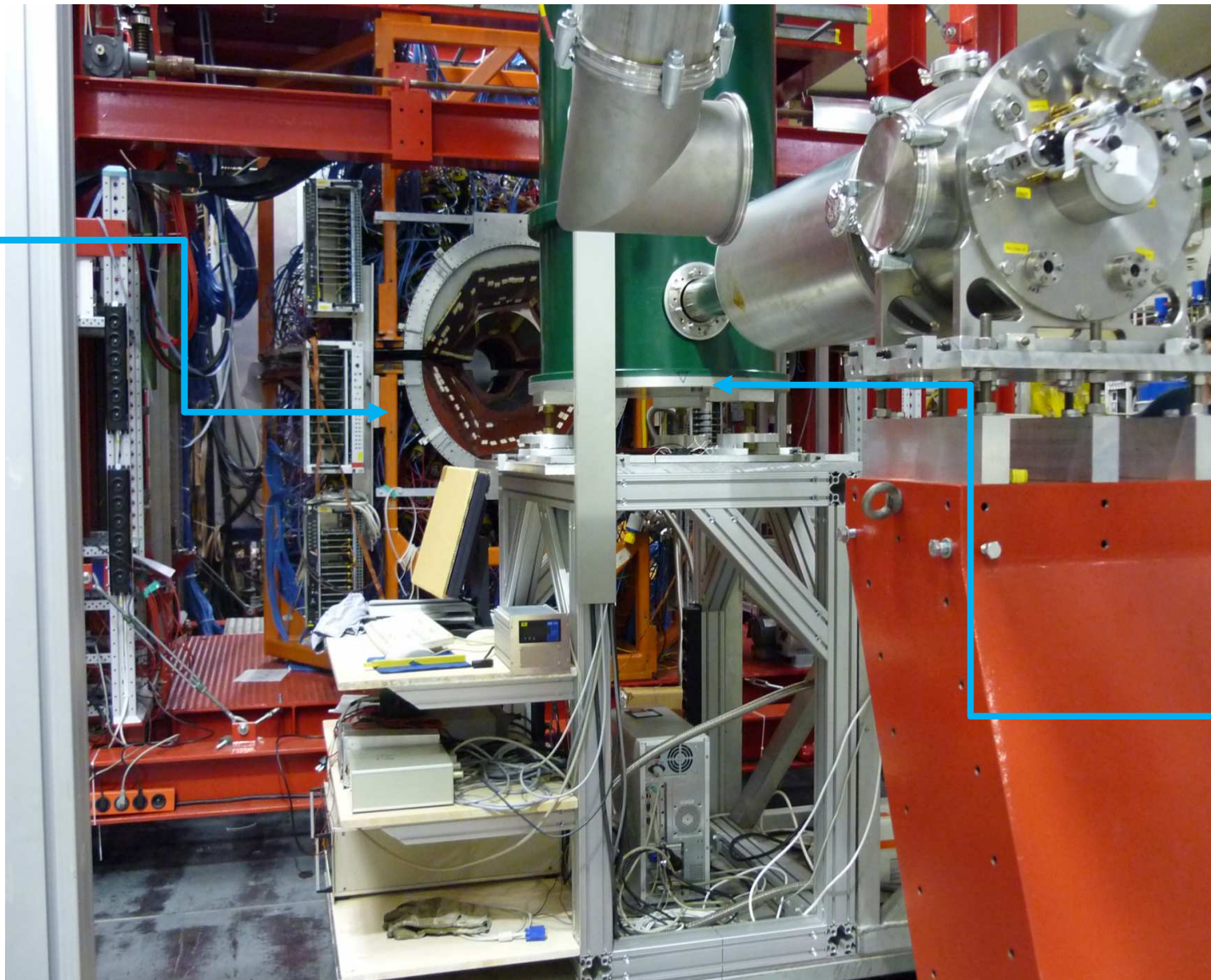
**Transverse (Saddle coil)**



**Longitudinal (Solenoid)**



**Internal  
Holding Field (1.2K, 0.6T)**



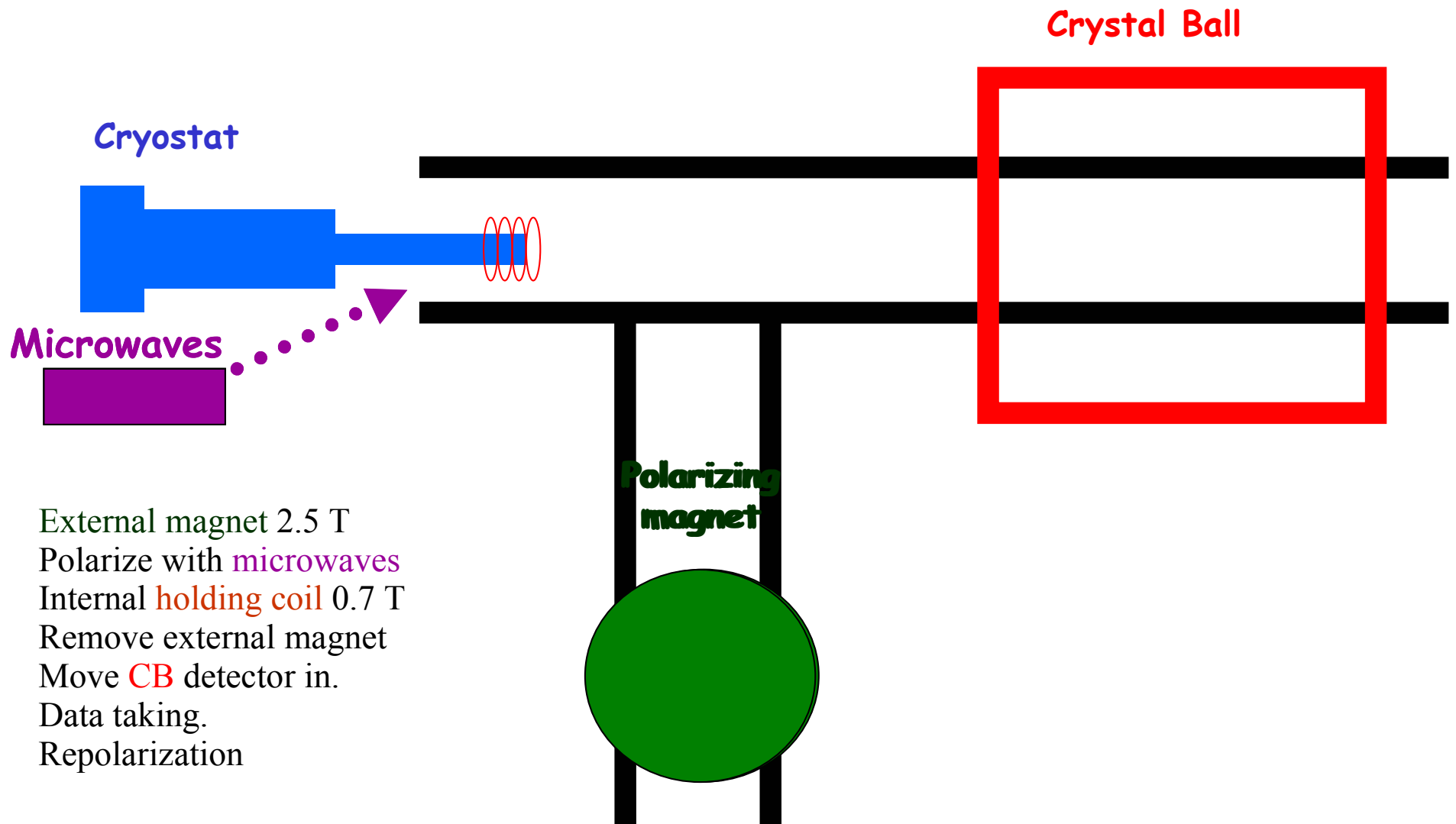
**Movable  
Crystal Ball  
4 $\pi$ -  
Photon  
Detector**

**Cryostat**

**Movable  
2.5 Tesla  
Polarizing  
Magnet**

First Beam with Transverse Polarization in December, 2009. Runs 2010 11.  
Longitudinal Polarization runs 2012, 2014, 2015.





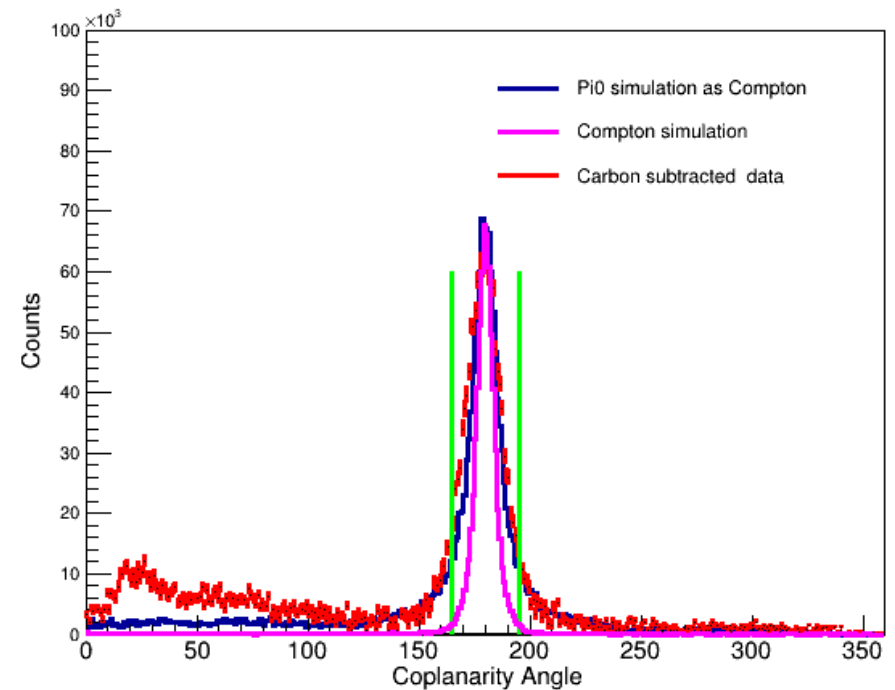
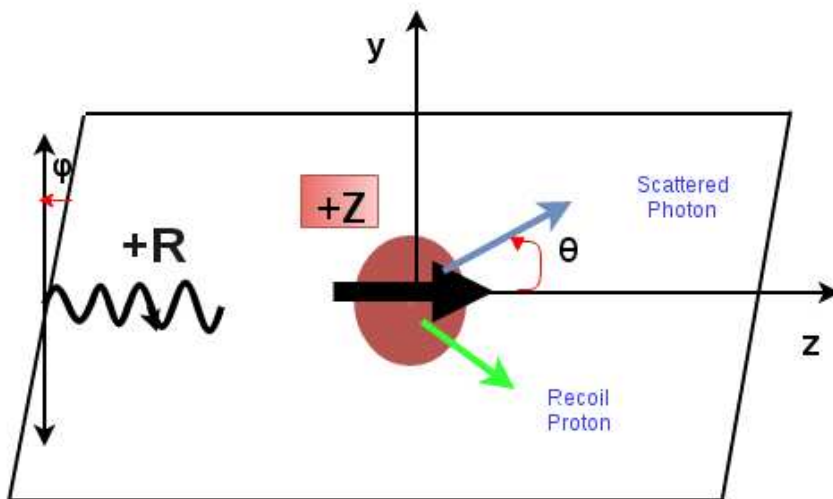
- **Small Compton scattering cross sections.**
- **Large backgrounds:**
  - $\pi^0$  photoproduction cross section is about *100 times* that of Compton scattering.
  - Coherent and incoherent reactions of C, O, He in polarized target.
- In  $\Delta$ -region, proton tracks can be used to suppress backgrounds,
  - but energy losses in the LH<sub>2</sub> target, frozen-spin cryostat, and CB-TAPS are considerable.
- Under certain conditions,  $\pi^0$  photoproduction can mimic Compton scattering.



# Compton Scattering Event Selection

- Momentum Conservation requires the reaction to be coplanar.
- Require ONLY one **neutral** and one **charged track**.
- Require a cut on Coplanarity Angle

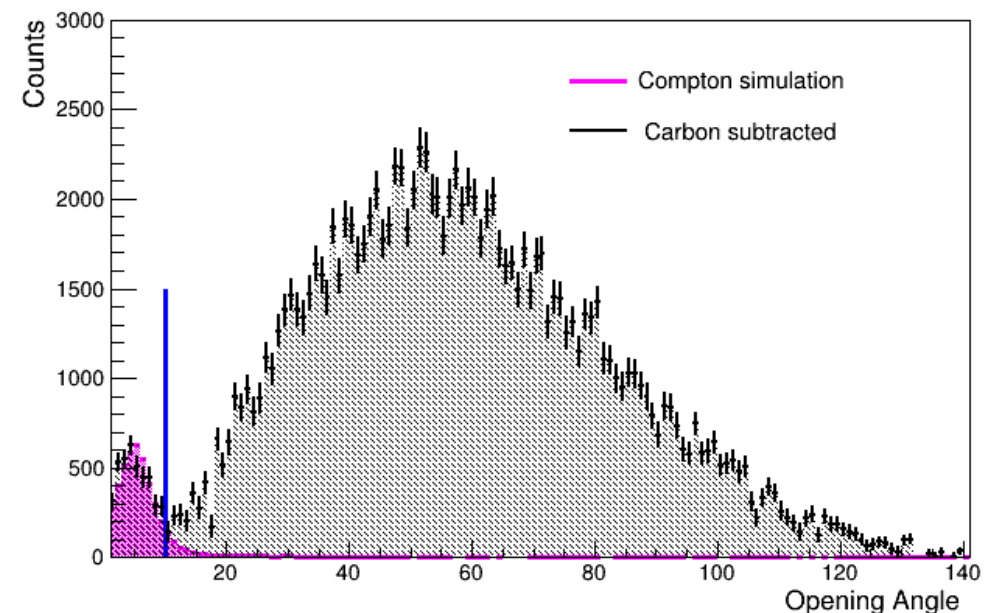
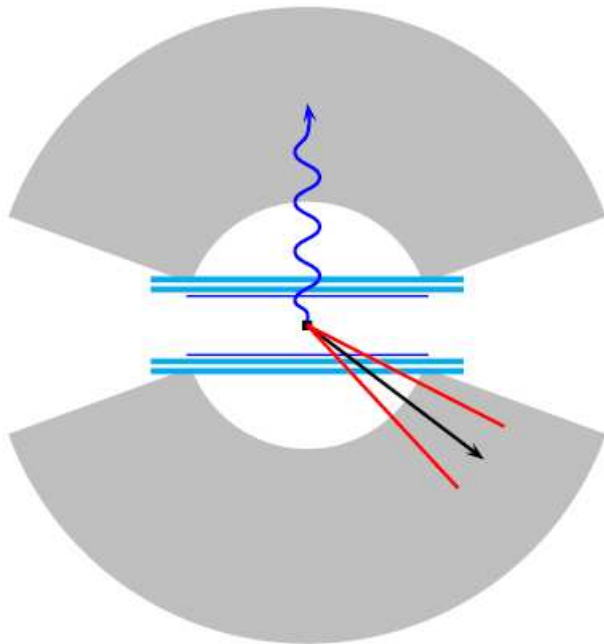
$$\Delta\phi = |\phi_{\gamma} - \phi_{\text{recoil}}| = 180^{\circ} \pm 15^{\circ}$$



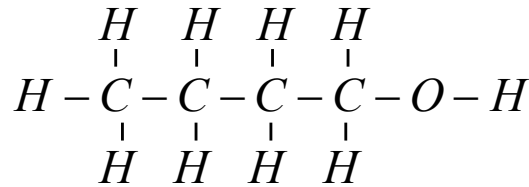
# Compton Event Selection (2)

- Use the detected photon information to calculate the **angle of the scattered proton**, and compare it to the **actual detected proton angle**.

$$\text{Opening Angle } \cos \Theta_{OA} = \frac{\vec{p}_{miss} \bullet \vec{p}_{recoil}}{|\vec{p}_{miss}| \times |\vec{p}_{recoil}|}$$



# Backgrounds from Butanol Target



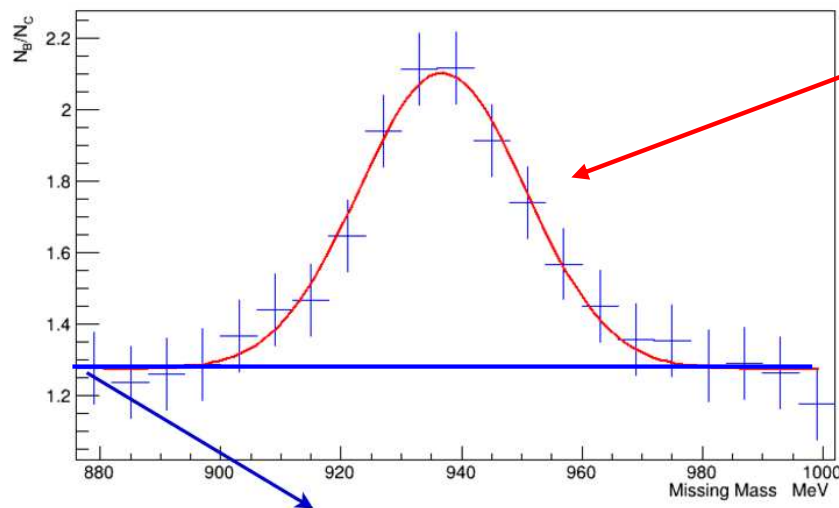
- **Butanol (C<sub>4</sub>H<sub>9</sub>OH)** doped with free electrons is needed for target material due to its large electron dipole moment.
  - Compton scattering off H
  - Coherent scattering off C,O
  - Incoherent scattering off C,O
  - Pion production off H
  - Coherent pion off C,O
  - Incoherent pion off C,O
- Backgrounds also arise from the liquid He cryogen.



- Density of carbon target is chosen to match the number of non hydrogen nucleons in the Butanol target.
- Dedicated carbon target runs taken for data subtraction.

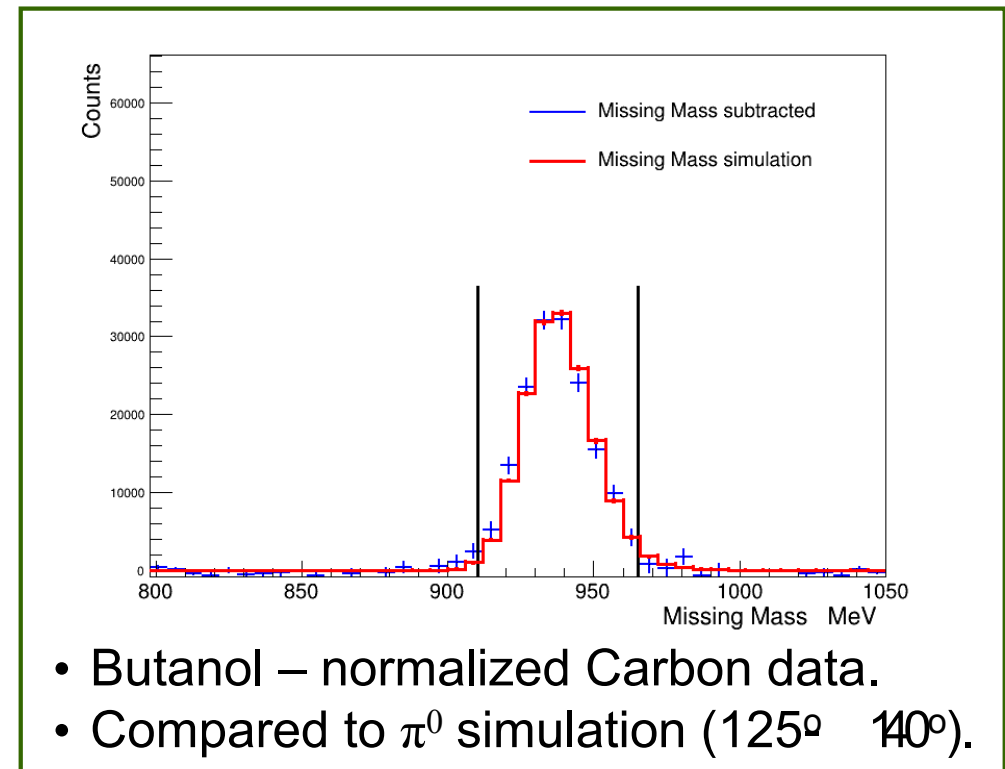
# $\pi^0$ Channel used for Carbon Target Normalization

- Butanol target data:
  - Detect ONLY two photons and reconstruct  $\pi^0 \rightarrow \gamma\gamma$ .
- Compute mass of undetected recoil nucleon.



Gaussian peak:  $\pi^0$  photoproduction off  $^1\text{H}$

- Constant background underneath is incoherent pion production off non  $^1\text{H}$  nucleons in butanol.
- Used to normalize carbon target data, together with live-time corrected tagger scalars.

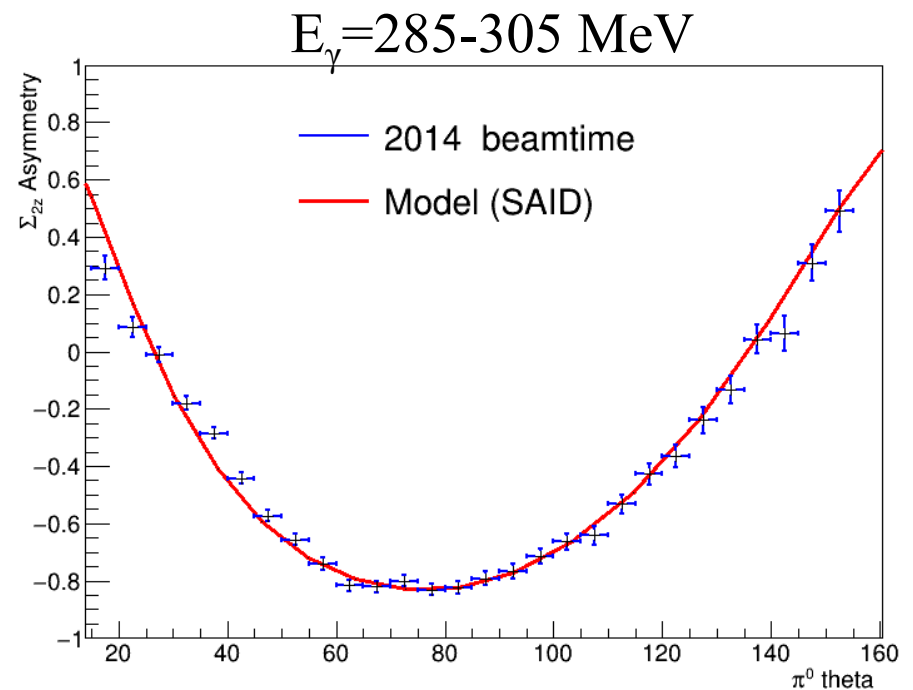
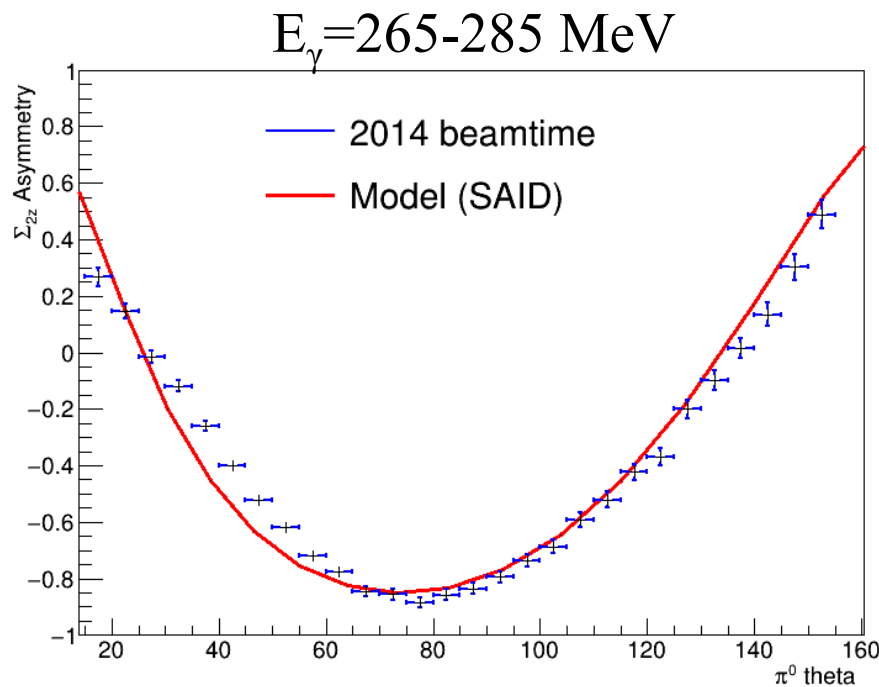


- Butanol – normalized Carbon data.
- Compared to  $\pi^0$  simulation ( $125^\circ$   $140^\circ$ ).

# Confirm with $\pi^0 \Sigma_{2z}$ Asymmetry

- Compute  $\Sigma_{2z}$  Asymmetry for  $\pi^0$  photoproduction.
- If non-H contributions are subtracted properly, the results should compare well to SAID isobar model.

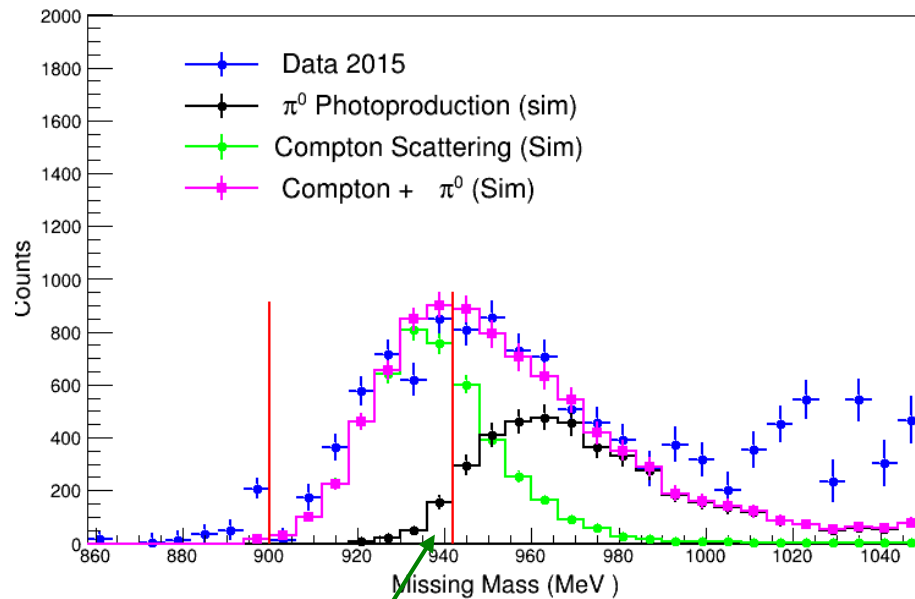
$$\Sigma_{2z} = \frac{1}{P_{circ}^\gamma} \left( \frac{(N_{+z}^R + N_{-z}^L) - (N_{+z}^L + N_{-z}^R)}{P_{+z}^t (N_{+z}^R + N_{-z}^L) - P_{-z}^t (N_{+z}^L + N_{-z}^R)} \right)$$





# Compton Event Selection (3)

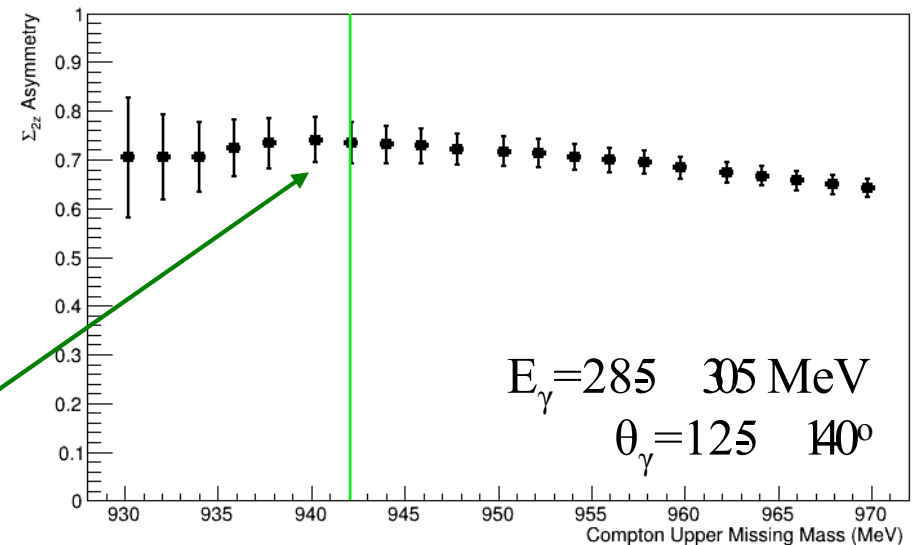
- Compute recoil mass for one **neutral** and one **charged track** data.



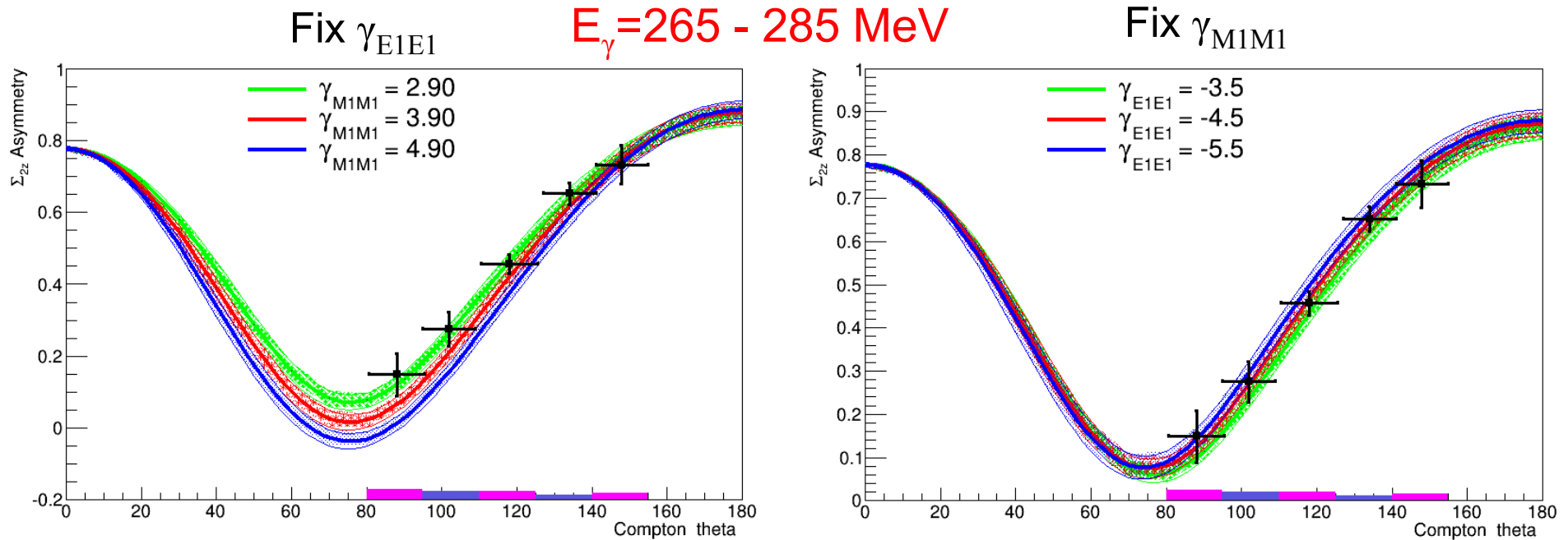
$$m_{miss} = \sqrt{(E_{\gamma i} + m_p + E_{\gamma f})^2 - (\vec{p}_{\gamma i} - \vec{p}_{\gamma f})^2}$$

$$= m_p$$

- To maximize statistics, compute  $\Sigma_{2z}$  for different  $m_{miss}$  cuts.
- Upper cut limit chosen at lower of:
  - Simulated  $\pi^0$  contamination <5%.
  - $\Sigma_{2z}$  varies by <5% from reference value.



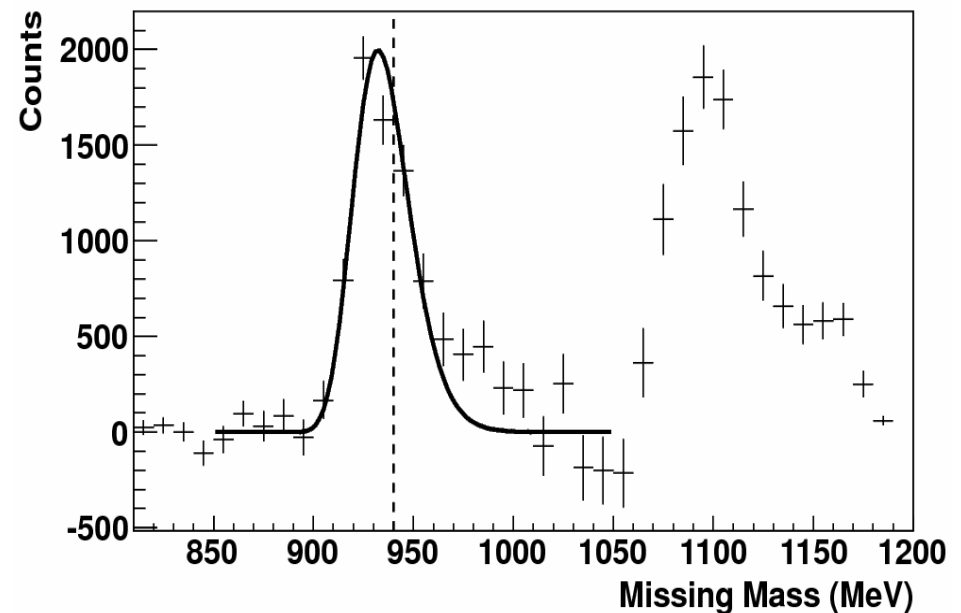
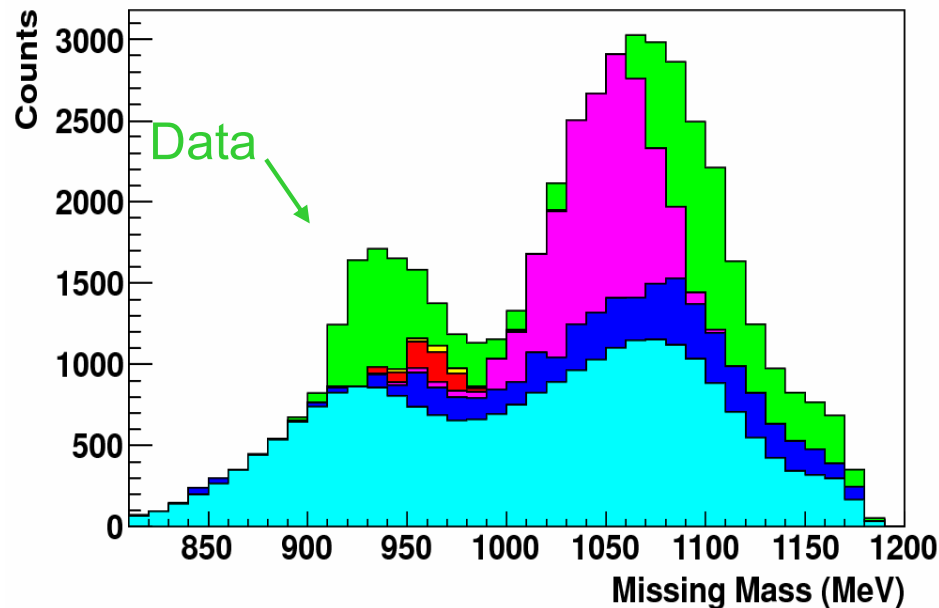
# Compton $\Sigma_{2z}$ Results



- Error bars include statistical and random systematic uncertainties.
- Correlated systematic uncertainties shown as blocks at bottom.
- Curves are from HDPV calculation of Pasquini et al., making use of constraints on  $\alpha_{E1} + \beta_{M1}$ ,  $\alpha_{E1} - \beta_{M1}$ ,  $\gamma_0$ ,  $\gamma_\pi$  (allowed to vary within experimental errors).
- Comparisons were also done with  $B\chi PT$  calculation of Lensky & Pascalutsa.
- $\Sigma_{2z}$  clearly sensitive to  $\gamma_{M1M1}$ , not very sensitive to  $\gamma_{E1E1}$ .

# $\Sigma_{2x}$ – Transversely Polarized Target

$E_\gamma = 273 - 303$  MeV and  $\theta_{\gamma'} = 100 - 120^\circ$



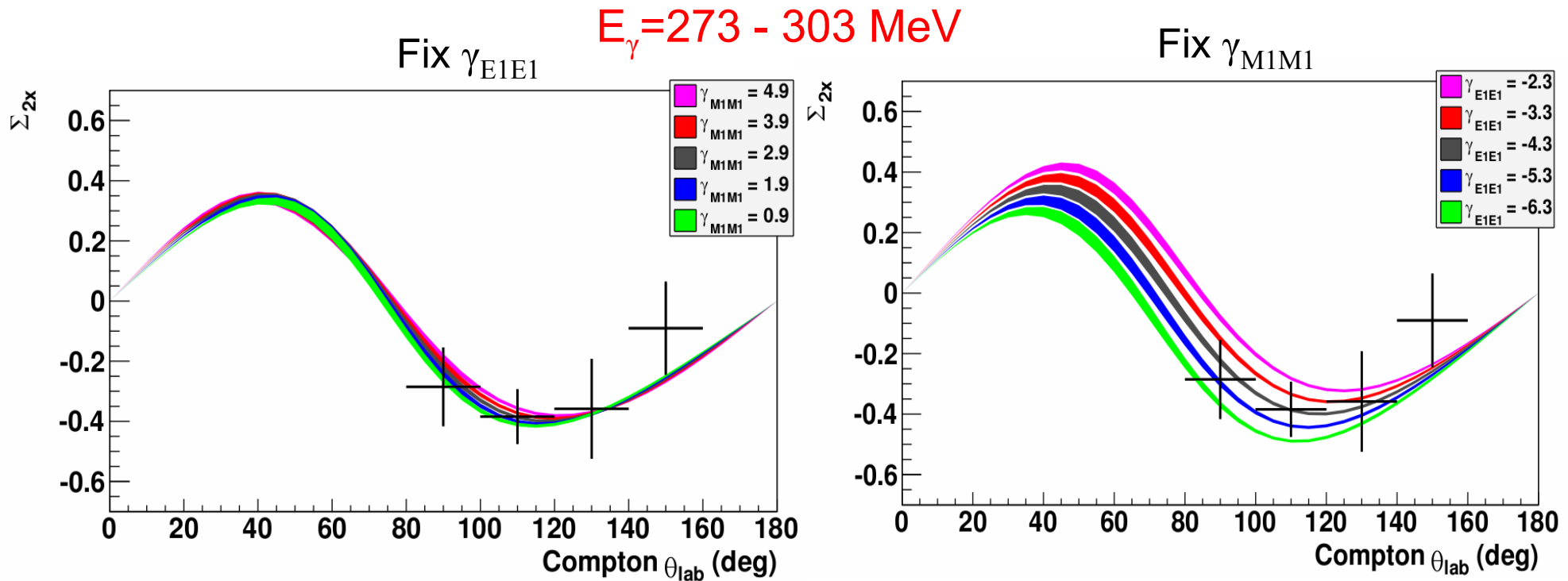
## Background contributions to MM:

- accidental coincidences
- carbon/cryostat contributions
- reconstructed  $\pi^0$  background where one decay  $\gamma$  escapes setup in:
  - TAPS downstream hole
  - CB upstream hole

## Fully subtracted MM spectrum:

- conservative MM < 940 MeV integration limit
- simulated Compton peak

# $\Sigma_{2x}$ – Transversely Polarized Target



- First measurement of a double spin Compton scattering asymmetry on the nucleon.
- Curves are from HDPV calculation of Pasquini et al., making use of constraints on  $\alpha_{E1} + \beta_{M1}$ ,  $\alpha_{E1} - \beta_{M1}$ ,  $\gamma_0$ ,  $\gamma_\pi$  (allowed to vary within experimental errors).
- Checks were done with  $B\chi$ PT calculation of Lensky & Pascalutsa.
- $\Sigma_{2x}$  clearly sensitive to  $\gamma_{E1E1}$ , not very sensitive to  $\gamma_{M1M1}$ .

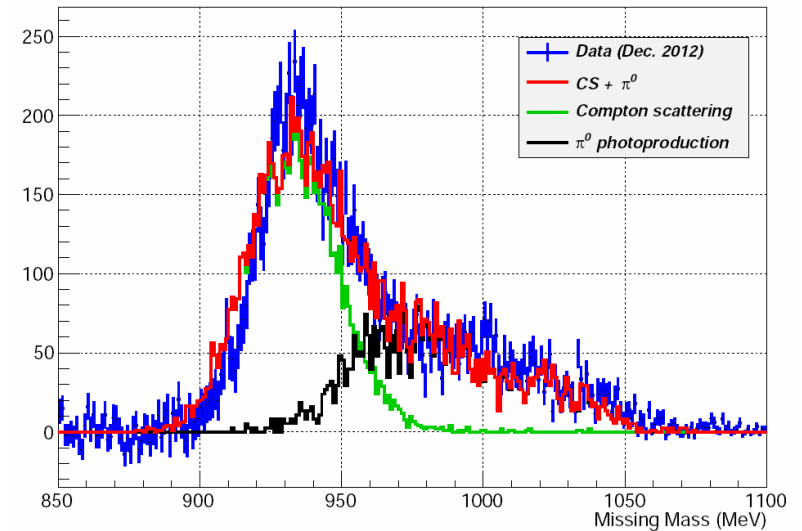
P. Martel et al., PRL 114 112501 (2015).

# $\Sigma_3$ above pion production threshold

Simulation of  $\pi^0$  photoproduction in LH<sub>2</sub> target matches background of the distribution quite well.



$E_\gamma = 273 - 303$  MeV and  $\theta_\gamma = 100 - 120^\circ$



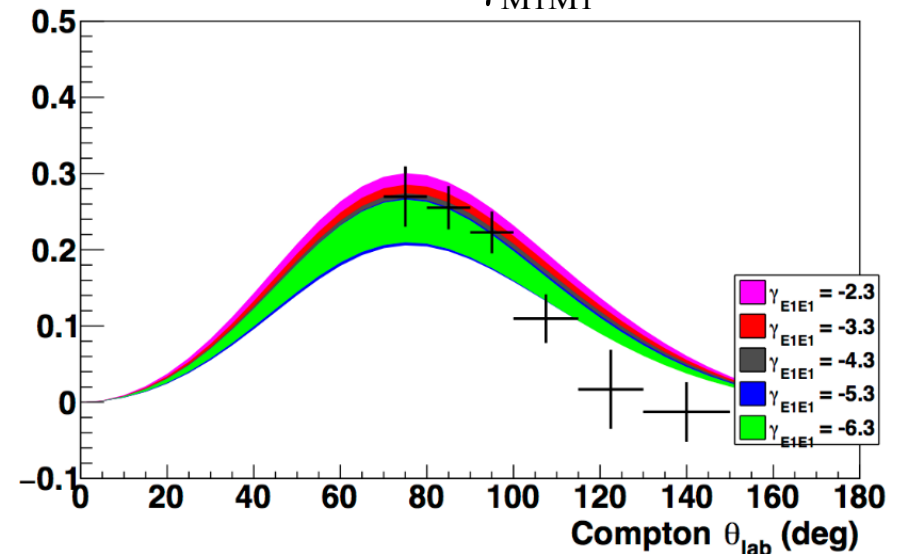
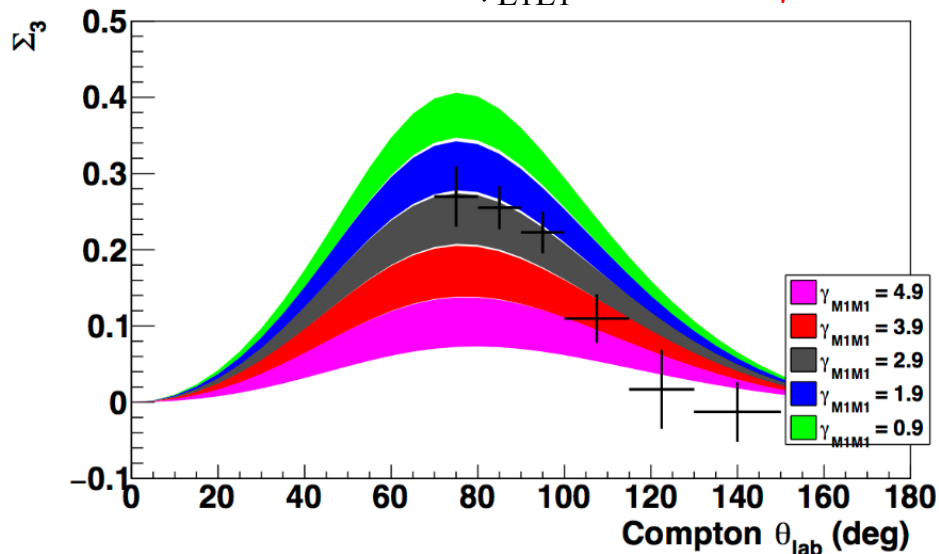
$\Sigma_3$  measurements along with HDPV calculation of Pasquini et al., making use of constraints on  $\alpha_{E1} + \beta_{M1}$ ,  $\alpha_{E1} - \beta_{M1}$ ,  $\gamma_0$ ,  $\gamma_\pi$  (allowed to vary within experimental errors).

Garth Huber, huberg@uregina.ca

Fix  $\gamma_{E1E1}$

$E_\gamma = 287 - 307$  MeV

Fix  $\gamma_{M1M1}$



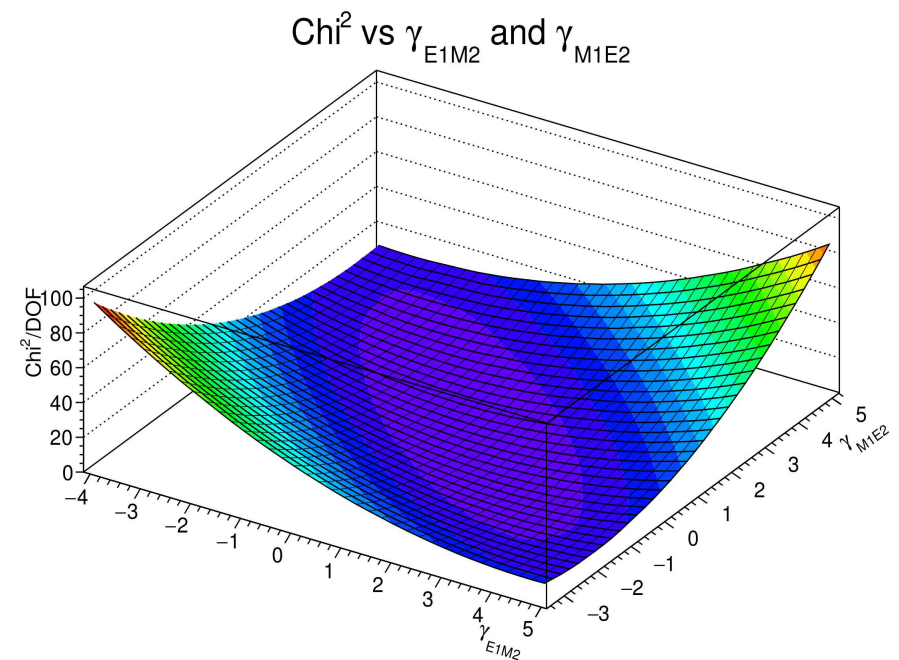
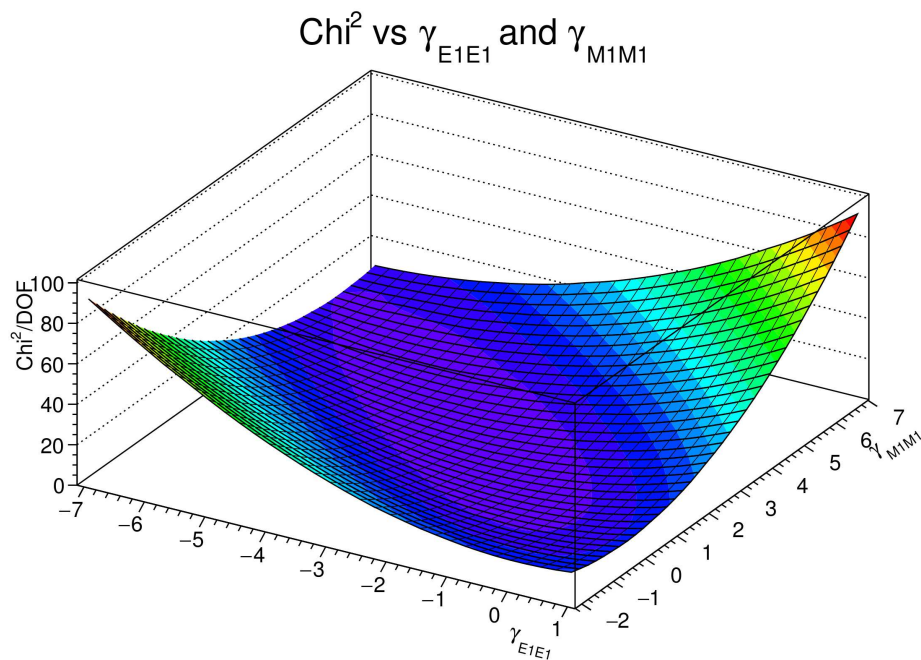


## ■ Global Fit:

- Includes MAMI results for  $\Sigma_{2Z}$ ,  $\Sigma_{2X}$ ,  $\Sigma_3$  and prior  $\gamma_0$ ,  $\gamma_\pi$ ,  $\alpha_{E1}$ ,  $\beta_{M1}$ .
- Goal is to extract all four spin polarizabilities independently with small statistical, systematic and model-dependent errors.

## • Fits done separately for:

- HDPV calculation of Pasquini et al. (shown below).
- $B_\chi$ PT calculation of Lensky & Pascalutsa (very similar).



- Dispersion relation and  $B\chi$ PT results are reasonably consistent.
- Pion pole contribution has been subtracted.

	HDPV Pred.	HDPV 2015 $\Sigma_{2x} + \Sigma_3^{MAMI}$	HDPV 2017 $+ \Sigma_{2z}$ Fit	$B\chi$ PT Pred.	$B\chi$ PT 2017 Fit
$\gamma_{E1E1}$	-4.3	-5.0±1.5	-4.24±0.39	-3.3	-2.87±0.42
$\gamma_{M1M1}$	2.9	3.13±0.88	3.25±0.40	3.0	2.29±0.39
$\gamma_{E1M2}$	-0.0	1.7±1.7	0.76±0.83	0.2	0.60±0.85
$\gamma_{M1E2}$	2.2	1.26±0.43	1.24±0.39	1.1	0.98±0.35
$\gamma_0$	-0.8	-1.00±0.18	-1.00±0.18	-1.0	-0.99±0.35
$\gamma_\pi$	9.4	7.8±1.8	7.98±1.36	7.2	5.54±1.25
$\alpha + \beta$		13.8±0.4	13.77±0.40		13.78±0.40
$\alpha - \beta$		6.6±1.7	7.29±0.86		6.76±0.87
$\chi^2/df$		1.25	0.83		1.30

Spin polarizabilities in units of  $10^{-4} \text{fm}^4$ .  
Scalar polarizabilities  $10^{-4} \text{fm}^3$ .

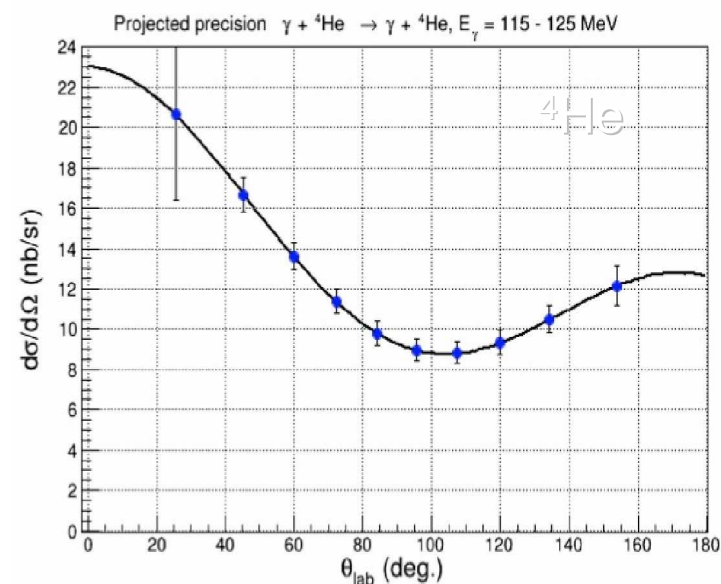
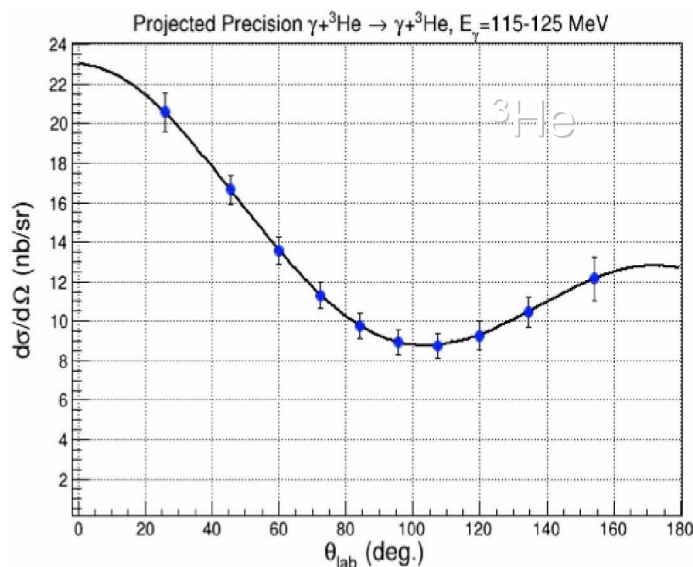
# Neutron Scalar Polarizabilities

In certain kinematic regions, proton acts like a spectator and scattering is done from neutron.

▪ A relatively new idea is to use  $^3\text{He}$  instead of  $^2\text{H}$  target:

→  $\chi^2$ PT calcs by Shukla, Nogga, Phillips [NP **A819**, 98 (2009)]

→  $\alpha_{E1}^n, \beta_{M1}^n$  determined from fit to Angular distributions vs. Energy



J. Annand has made a high-pressure active  $^3\text{He}$  gas scintillator target.

- Proposal A2 0 2013 for  $^3\text{He}(\gamma, \gamma)^3\text{He}$  given 'A' rating by PAC.
- Expected good separation of backgrounds from target windows and  $\pi^0$  production.

**Polarizabilities are an important tool for testing QCD via  $\chi$ PT and DRs in the non-perturbative regime.**

- $\Sigma_{2x}$ ,  $\Sigma_{2z}$  have been measured for the first time.
  - Plans to acquire more  $\Sigma_{2x}$  data, but not yet scheduled.
- $\Sigma_3$  data taken to supplement existing data from LEGS.
  - Additional  $\Sigma_3$  data taking below pion threshold for  $\alpha_{E1}$ ,  $\beta_{M1}$  underway.

## Global Analysis Results:

- Uncertainties in  $\gamma_{E1E1}$ ,  $\gamma_{M1M1}$ ,  $\gamma_{E1M2}$  improved by factors of 2-4, uncertainty in  $\gamma_{M1E2}$  remained unchanged.

## Future:

- Implement active target to expand kinematic range.
- Extend measurements to neutron.





# Systematic Uncertainties

## Correlated Systematic Uncertainties

→ Added in Quadrature and shown as Blocks in Fig.

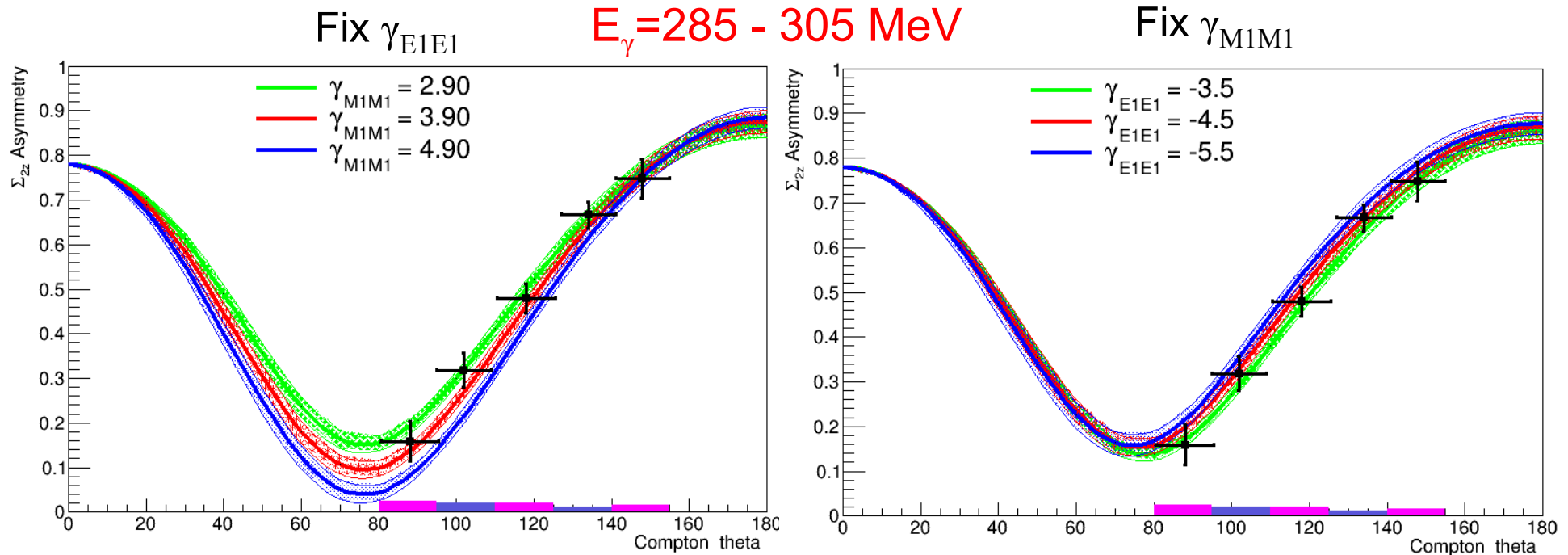
Target Polarization	$\pm 2\%$
Photon (Electron) Beam Polarization	$\pm 1\%$
Carbon Target Scaling Factor	$\approx \pm 8-12\%$

## Random Systematic Uncertainties

→ Added in Quadrature to the Statistical Uncertainties

Cuts on reconstructed proton missing mass	$\approx \pm 10\%$
---	--------------------

# Compton $\Sigma_{2z}$ Results



- Error bars include statistical and random systematic uncertainties.
- Correlated systematic uncertainties shown as blocks at bottom.
- Curves are from HDPV calculation of Pasquini et al., making use of constraints on  $\alpha_{E1} + \beta_{M1}$ ,  $\alpha_{E1} - \beta_{M1}$ ,  $\gamma_0$ ,  $\gamma_\pi$  (allowed to vary within experimental errors).
- Comparisons were also done with  $B\chi PT$  calculation of Lensky & Pascalutsa.
- $\Sigma_{2z}$  clearly sensitive to  $\gamma_{M1M1}$ , not very sensitive to  $\gamma_{E1E1}$ .